Employing Remote Sensing, Data Communication Networks, AI, and Optimization Methodologies in Seismology

Mohamed S. Abdalzaher, *Senior Member, IEEE*, Hussein A. Elsayed, *Member, IEEE*, and Mostafa M. Fouda, *Senior Member, IEEE*

***Abstract*—Seismology is among the intrinsic sciences that strictly affect human lives. Many research efforts are presented in the literature aiming at achieving risk mitigation and disaster management. More particularly, modern technologies have been employed in such a pivot. However, the day-to-day challenges and complexities of such natural science that face the stack holders still need more reliable and intelligent solutions. The solution can depend on a partial or integrated system of modern technologies. In this article, we extensively survey the corelated modern technologies aiming to gather the major efforts exerted in this regard. It also outlines the desirability of seismology to modern technologies. Then, we present a detailed analysis of remote sensing and data communication networks (DCNs), which are considered the backend of seismic networks. Furthermore, for seismology, we depict both classical and nonclassical approaches based on DCN principles, such as optical fiber-based acoustic sensors, social media, and the Internet of things (IoT). Following that, a comprehensive description of the various optimization techniques utilized for seismic wave analysis and for prolonging network lifetime is offered. A description of the important functions that artificial intelligence (AI) can play in different fields of seismology is also included. Finally, we present some recommendations for stack holders to prevent natural calamities and preserve human lives.**

***Index Terms*—Data communication networks (DCNs), deep learning, Internet-of-things (IoT), machine learning, optimization techniques, seismology, social media.**

I. Introduction

DUE to the nature of the earth's complex structure, it has to be effectively studied and how it is composed of. This complex structure produces a nonhomogeneity between the different earth layers' interconnection. Accordingly, such a type of interconnection brings out earthquakes (EQs) as a result of the produced seismic waves moving into the earth's layers. Consequently, an inevitable science called *seismology* is acquainted with that phenomenon and the corresponding aspects regarding the moving seismic waves throughout the earth [1], [2].

EQs are complex natural phenomena that require an interdisciplinary approach to be monitored, including using tools from physics, computer science, mathematics, electronic engineering, and others. More particularly, the data communication networks (DCNs)-based modern systems are considered the most supportive technology to the seismic network that can be used to observe seismic signals, transmit the seismic signals, and handle the interconnection between the engineering role and the seismological one. DCNs are not only limited to offering practical information about the seismic network and seismic waves, but also can be used in earthquake early warning system (EEWS), disaster management, and reducing seismic hazards and risk mitigation of the EQ-prone regions [3], [4].

The DCNs-based modern systems can provide a warning of strong shaking in advance, have a swift processing time, and is useful for blind zones where the target site is too close to the seismic source to obtain advanced warning by any currently available detection techniques [5], [6].

The site-specified network approach consists of multiple stations located at the target site and provides local warning of strong shaking based on the peak amplitude of the early P-wave signal. The prominent role of DCNs-based modern systems is to facilitate the warning message via different communication techniques [7], [8]. Besides, DCNs can effectively employ road networks to manage the EQs disasters and mitigate the consequent crises [4]. The DCNs can also provide low latency communications for the far seismic stations leading to prompt event detection. Therefore, a longer warning time at distant sites can be achieved.

It is worth noting that the DCN elements are used to estimate source parameters and then predict the shaking intensity at distant sites of interest, using regional ground motion and site amplification models. This allows issuing advance alerts for multiple locations that may experience strong ground vibration [9]. Besides, artificial intelligence (AI) can contribute to hazard assessment [10] and EQ discrimination [11].

Manuscript received 15 June 2022; revised 7 October 2022; accepted 21 October 2022. Date of publication 25 October 2022; date of current version 9 November 2022. *(Corresponding author: Mohamed S. Abdalzaher.)*

Mohamed S. Abdalzaher is with the Department of Seismology, National Research Institute of Astronomy and Geophysics, Cairo 11421, Egypt (e-mail: msabdalzaher@nriag.sci.eg).

Hussein A. Elsayed is with the Department of Electronics and Electrical Communications Engineering, Ain Shams University, Cairo 11566, Egypt (e-mail: helsayed@eng.asu.edu.eg).

Mostafa M. Fouda is with the Department of Electrical and Computer Engineering, Idaho State University, Pocatello, ID 83209 USA (e-mail: mfouda@ieee.org).

Digital Object Identifier 10.1109/JSTARS.2022.3216998

TABLE I
LIST OF ABBREVIATIONS

Abbreviation	Description	Abbreviation	Description
DCN	Data communication networks	CSMA/CD	Carrier sense multiple access with collision detection
IoT	Internet of things	DAS	Distributed acoustic sensing
AI	Artificial intelligence	CSMA/CD	Carrier sense multiple access with collision detection
EQ	Earthquake	HDBSCAN	Density-based spatial clustering of applications with noise
QB	Quarry blast	PV	Path vector
SDN	Software-defined network	SAMS	Seismic activities monitoring and analysis system
LTA	Long-term average	S and US	Supervised and Unsupervised
STA	Short-term average	DRS	Disaster recovery system
SNR	Signal to noise ratio	SNs	Sensor nodes
AIC	Akaike information criterion	NLOS	Non line of sight
TDMA	Time division multiple access	PGA	Peak ground acceleration
TS	Time slot	SDR	Source to distortion ratio programming
LOS	Line-of-sight	ML	Machine learning
LAN	Local area network	DL	Deep learning
EEWS	Earthquake early warning system	PPV	Peak particle velocity
LFS/LFR	Last frame sent/received	DAE	Deep auto encoder
SWS/RWS	Send/Receive window size	DNN	Deep neural network
UDP	User datagram protocol	DCNN	Deep convolutional neural network
TCP	Transmission control protocol	AP	Affinity propagation
RIP	Routing information protocol	HVSR	Horizontal-to-vertical spectral ratio
DV	Distance vector	SVM	Support vector machine
IGRP	Interior gateway routing protocol	LSTM	Long short term memory
EIRGP	Enhanced interior Gateway Routing Protocol	ANFIS	Adaptive neuro-fuzzy inference system
OSPF	Open shortest path first	PSO	Particle swarm optimization
IS-IS	Intermediate system to Intermediate system	SWARA	Step-wise assessment ratio analysis
BGP	Border gateway protocol	GWO	Gray wolf optimization

On the other hand, dominant mathematical means are inevitable to be used in seismology, such as optimization techniques. The optimization can be effectively utilized in seismic waves' analysis, detection, inversion, prolonging the seismic networks' lifetime, securing the seismic data, enhancing the seismic waves' link transmission, and exploiting other existing resources to support seismic stations and their data transmission, etc.

In this article, an extensive view is presented about the dependence of seismology on modern technologies, such as DCNs, AI, optical fiber, Internet-of-things (IoT), and optimization techniques. Moreover, various currently available DCN approaches are covered in this article, and each should be considered taking into account the nature of the region and the desired objectives. These approaches can be used individually or combined to provide the best possible solution. Besides, the nominated optimization techniques for seismology and the interdisciplinary are surveyed. Finally, the article is summarized and future trends are presented. Table I lists the abbreviations used throughout the article. Our extensive survey is unique because of the study of the integration of remote sensing, DCNs, optical fiber, IoT system, social media, AI, and optimization techniques for attaining an efficient EEWS that can be established over three phases (deploying alarm, disaster management, and risk mitigation). Fig. 1 depicts the involved modern technologies and methodologies employed in seismology throughout the presented study.

The article's structure is portrayed as follows. Section II presents an overview of the desirability of seismology to modern technologies. Section III indicates the role of remote sensing in seismology. Then, Section IV introduces an extensive study of DCNs that serve seismic networks. Section V portrays the classical and nonclassical methodologies relying on DCN concepts for seismology. Afterward, in Section VI, we present an extensive overview of various optimization techniques that are used for seismic wave analysis and for prolonging the networks' lifetime. Section VII summarizes the significant roles that AI can play in different disciplines in seismology. Finally, Section VIII concludes this article.

II. OVERVIEW OF SEISMOLOGY AND DESIRABILITY TO MODERN TECHNOLOGIES

An EQ or an explosion can cause an elastic wave known as a seismic wave. Rayleigh and Love waves are two types of seismic waves that can travel through the interior of the earth as well as along its surface (P and S waves) [12], [13]. These waves can be analyzed in some cases to explore what the earth hides (such as monument areas, nonrenewable energy sources, and caves) and to investigate the shallow subsurface structures. Generally speaking, raw seismic data contains two main sources. First, the waves that are generated from the inner earth layer result from EQs, volcanic eruptions, magma movement, and large landslides. Second, artificial waves are those produced by humans, typically on a surface that has been carefully built or in a pool.

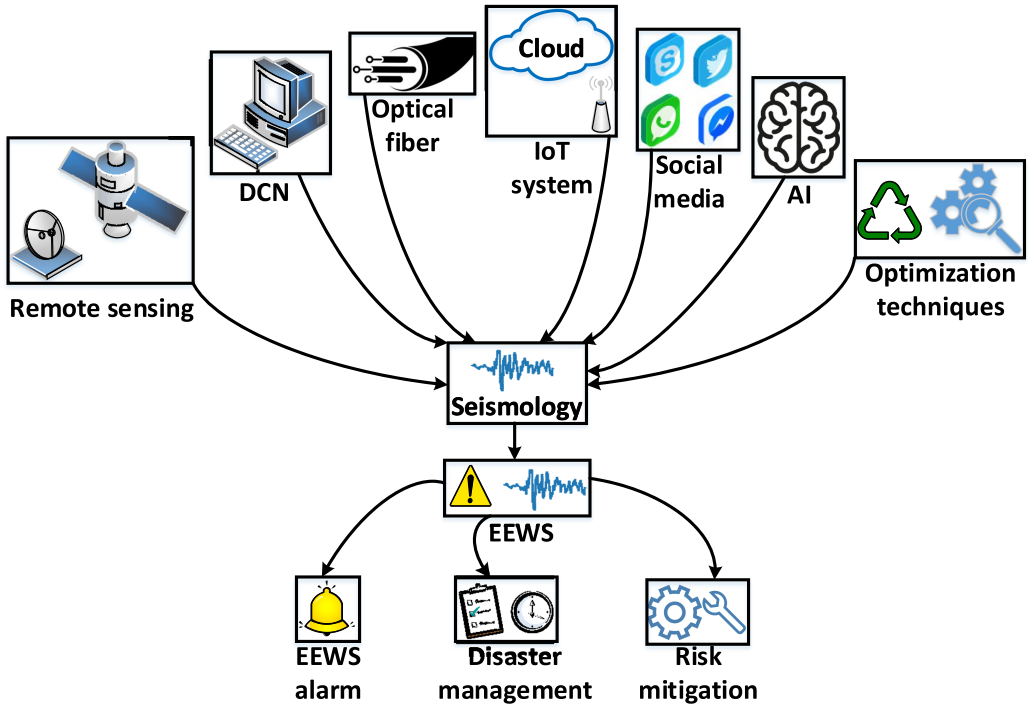

Fig. 1. Effective modern technologies and methodologies employed in seismology.

The EQ waves are distinguished by low-frequency acoustic energy and low amplitude that can be recorded by a seismometer, hydrophone (in water), or accelerometer. The velocity of those waves is observed by the seismometers, while the strong motion (acceleration) is measured by the accelerometers. The signal propagation velocity and acceleration depend on the density and elasticity of the three main earth layers (i.e., core, mantle, and crust). The velocity is directly proportional to the depth, where it ranges from 2 to 8 km/s in the crust layer and up to 13 km/s in the deep mantle [12], [13].

Using different seismic stations' records for the same event significantly assists the seismologist in accurately determining the EQ source epicenter and hypocenter. The epicenter contains the latitude and longitude of the observed EQ signal source, while the hypocenter reveals the depth of that source. The EQ event distances are fundamentally classified into three main types, namely, local, regional, and teleseismic, where the nearest EQs represent the local followed by regional and then the teleseismic.

The classical algorithms of the seismic waves detection and analysis are based on time-series analysis involving long-term average (LTA), short-term average (STA), and Akaike information criterion (AIC) [14], [15]. The LTA represents the slow trend of the EQ signal energy, while the STA is more responsive to a sudden increase in that energy. The ratio of STA/LTA is utilized to measure the signal-to-noise ratio (SNR). If this ratio exceeds a specific threshold, the EQ time is detected. Accordingly, the EQ monitoring system starts to calculate the hypocenter of the event once some seismometers observed that event. Notice that, the time window length of LTA and STA depends on the average distance to the most active seismic region and the distance between the receivers. The LTA period is longer than a group of a few identical seismic noise fluctuations, while the STA period is longer than a group of a few identical seismic signals. AIC can be applied to a single component of the observed event to provide an effective time estimate, where generally, the observed seismic waves consist of three components. Therefore, AIC has been widely utilized for picking the onset time of the seismic wave [15].

In [16], a listric fault detection method is proposed to pinpoint the harmful consequences of petroleum and gas exploration in the earth's crust due to this fault type. The authors in [16] proposed an interpretation work process based on a texture of major listric faults in a 3-D migrated seismic volume. Moreover, a 3-D texture gradient is calculated. The calculation depicts the contrast between neighboring cubes to every voxel in a seismic volume over depth or time, inline directions, and crossline. Then, an adaptive global threshold is computed to be applied to the 3-D volume map to acquire a binary map that addresses the potential of the listric faults boundary regions. In [17] and [18], the authors exploit the image processing techniques for interpreting the seismic structure. Those techniques are utilized to figure out faults, salt domes, and geologic structures.

The seismic networks are acquainted with observing the seismic wave as a real-time application 24/7. In such networks, the utilized system is mainly based on the DCN elements, mechanisms, protocols, etc., for data observation, transmission, and saving. After that, the role of data analysis comes, in which the observed raw data is filtered and analyzed to be able to detect the event's parameters such as latitude, longitude, depth, and magnitude. This role relies on the accurate detection of the incoming P-wave and S-wave of the same event from different

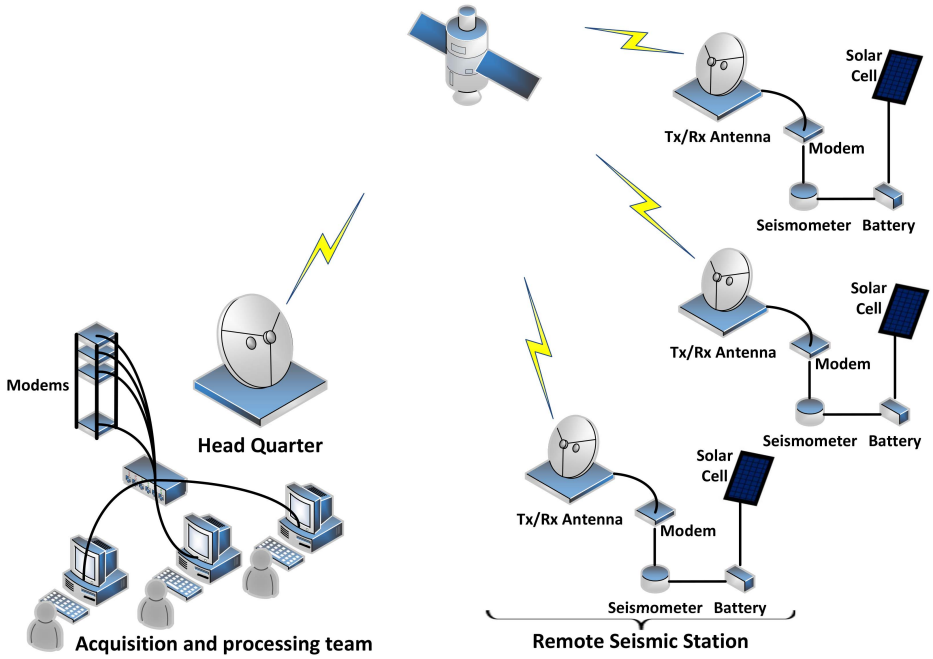

Fig. 2. General seismic observation system diagram.

TABLE II
HARDWARE EQUIPMENT AND THEIR FEATURES

Hardware equipment	Type	Manufacturer	Main features
Trillium	Seismometer	Nanometrics Co.	EQ speed measurement
Centaur	Digitizer	Nanometrics Co.	Convert the observed analog signal to digital
Cygnus	Outdoor modem	Nanometrics Co.	Transceiver
Carina	Indoor modem	Nanometrics Co.	Transceiver
Titan	Accelerometer	Nanometrics Co.	EQ acceleration measurement

stations. It is worth noting that the larger the number of observing stations to the same event is, the more accurate the event parameters calculation is.

Fig. 2 shows the utilized system diagram for observing the seismic data and then sending them to be analyzed at the data center relying on remote sensing tools. The system consists of hardware and software components as follows. It is worth mentioning that the team for the acquisition and processing of seismic signals should be well-trained and expert enough to work on a such vulnerable system. More particularly, this team is first involved in determining the efficiency of the observed seismic data. Second, they are in charge of performing important processing on this data such as picking, denoising, discrimination, etc. In this regard, both remote sensing, DCN, AI, and optimization techniques can play significant roles in seismic parameter calculations, hazard assessment, and disaster management.

A. Hardware Components

The hardware components in such a system implement several functions including seismometers, digitizers, outdoor modems, indoor modems, and accelerometers. Samples of these components are listed in Table II with brief information about them.

Mostly, seismic networks are involved in observing all the seismic activities whether local, regional, or teleseismic ones. The local events are the ones that occur within the country area, while the regional events are outside the country area but still on the same continent. The tele event is the one that occurs in a different continent that is very far from the country area. There are commonly used seismic network infrastructures, i.e., leased lines, line-of-sight (LOS)-based microwave signals, and satellite communication.

B. Software Components

The software collects the information from the distributed seismometers through the communication links and then processes it to extract the required signal from the raw data including the noise with manual analysis. The software role can contribute to effectively determining the data lost (gaps) along with the distributed DCN elements in the allocated seismic network stations.

Once again, DCN can contribute to efficiently retrieving the lost data of the observed seismic data. The utilized DCN elements and communication mechanisms can pinpoint the data gaps and smoothly extract them from the memories of the employed equipment in a safe way. Then, this data is well organized

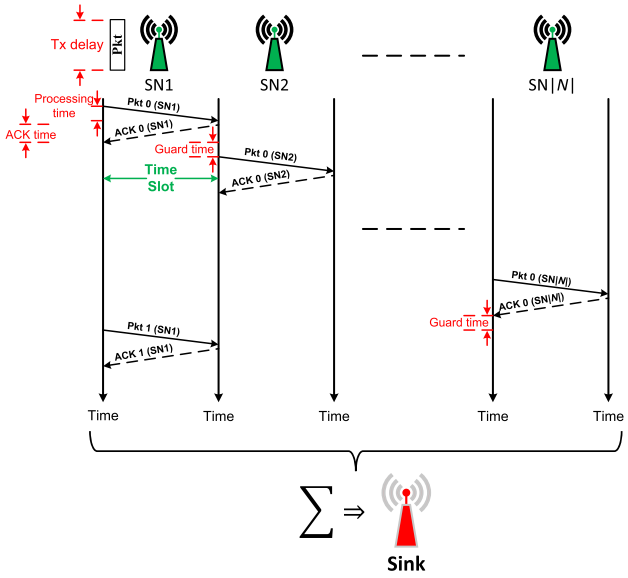

Fig. 3. TDMA slots distribution.

and retransmitted relying on an efficient media access technique such as time division multiple access (TDMA) to determine which packet/(s) is/are lost and from which station should be retransmitted.

The TDMA mechanism utilized in those observatories for transmitting the observed signal from stations and retrieving the gaps of the data lost once again is based on sequence numbers/time slots (TS) given to participant stations. This sequence can be illustrated in Fig. 3.

III. Remote Sensing in Seismology

Remote sensing is among the fast-booming modern technologies that effectively contribute to the seismology field. It is not limited to the terrestrial devices employed for the direct observations of the earth's crust layer but also extended to the satellite systems. Recently, climate change has been considered as a potential indicator for indicating EQ where remote sensing can be effectively used [19], [20]. In the literature context, remote sensing has been utilized for seismology in several research efforts such as thermal activity detection, detecting tropospheric ozone anomaly preceding strong EQs, ionosphere magnetic field anomaly associated with powerful EQs, etc.

Using the indicator of ozone anomaly, the tropospheric ozone before and after the 2008 Wenchuan EQ was examined in [21]. For 18 years from 2003 to 2020, the atmospheric infrared sounder ozone volume mixing ratio at various pressure levels (600, 500, 400, 300, and 200 hPa) has been taken into consideration to find the distinctive behavior connected with severe EQs. According to the findings, there was a noticeable increase in tropospheric ozone five days before the major event, which was dispersed around the Longmenshan fault zone. In this regard, many factors such as focal mechanism, focal depth, tectonic environment, geological environment, meteorological conditions, etc., are all thought to play a role in the unusual behavior of tropospheric ozone. This was supported by the observation of an increase in the index of ozone anomaly around the time of the 2013 Lushan and 2017 Jiuzhaigou EQs. The position of elevated tropospheric ozone serves as an EQ epicenter indicator. Accordingly, one of the key elements influencing the emergence of abnormal tropospheric ozone may be the EQ's size.

Interestingly, aerial remote sensing images have been employed for landslide mapping. In [22], a suggested method for creating a landslide inventory map using extremely high-resolution remote sensing images has been successfully tested on real datasets of landslide locations in Lantau Island of Hong Kong, China. Unlike the classical approaches, that paper exploited the bitemporal very high-resolution exported by the images of remote sensing without producing the map of change magnitude.

The authors in [23], showed how consistent nighttime light imagery from the Defense Meteorological Satellite Program's Operational Linescan System can be used to analyze EQ resistance at the county level. To analyze the static and dynamic adaptability of various counties, they first created an EQ stability model using a nighttime light index. They then intercalibrated the nighttime light data and calculated the sum of all stable lights for each of the 261 counties impacted by the Mw 7.9 Wenchuan EQ from 1992 to 2013. Finally, they investigated the potential affecting elements from geographic, disaster perspectives, socioeconomic standpoints, and political aspects. First, the findings demonstrated that the static flexibility of the severely damaged counties in the affected area due to Wenchuan EQ that increased from south to north along the long axis of the intensity zone, and plain and protoplasmatic counties demonstrated a quicker short-term economic recovery than plateau and mountainous counties. In addition, all counties that were particularly heavily damaged, except Wenchuan, Dujiangyan, and Pingwu, returned to normal by 2011, whereas 52% of the counties in the areas that were generally affected did so in less than three years. Furthermore, the authors discovered via linear regression that socioeconomic aspects, e.g., the allotting of population age, industrial structure, and social welfare are probably connected to the danger of soil liquefaction, average elevation, degree of land usage, and EQ resilience.

In [24], the passive microwave employed in remote sensing has been utilized for detecting the temperature anomaly associated with strong EQs. More particularly, the authors have concentrated on the areas with raising soil moisture in Sichuan province, China. The study explored a prior microwave radiation anomaly index to three powerful EQs in Wenchuan with a magnitude (Mw = 7.8), Lushan with a magnitude (Mw = 6.6), and Jiuzhaigou with a magnitude (M = 6.5) from 2008 to 2018 based on the satellite data (Microwave Imager). The obtained results indicated that the anomaly of microwave brightness temperature has been observed two months preceding these three EQs.

The role of satellite imaging has been also extended using a mapping of two independent hybrid open-pit mining along with Gaofen-2 [25]. That work planned the confronting issues to the mapping of hybrid open-pit mining areas because the complex types of landscapes led to low accuracy. Consequently, that work employed satellite images with high spatial resolution. The results proved that this model could map 111 open-pit mine sites.

Due to the day-to-day challenges facing remote sensing, an intelligent satellite solution is desired. The authors in [26] highlighted the efforts exerted in developing an intellectual solution for the remote sensing satellites. More concretely, they considered the main key technologies such as onboard processing systems and payloads of images. They have classified them into pros and cons based on the information exchanged between remote sensing satellites and terrestrial devices.

The authors in [27] offered enhancements to the two-step approach previously published to recover seismic microwave brightness temperature anomaly and devised a novel method known as spatiotemporally weighted about the first law of geography and its extension in the time domain. Nonseismic data were used to determine the temporally weighted background, which was then applied to eliminate the long-term trend to recover the fundamental microwave brightness temperature residuals. To recover cleaned microwave brightness temperature residuals, a spatially weighted background has been created based on Euclidean geographical distance from the epicenter and utilized to remove local meteorological noise.

In [28], the approach of background field analysis has been employed. That model concentrated on statistically processing radiation the data's worth and the tidal force fluctuant analysis approach, which uses the impact of tidal oscillations to get small changes in radiation after abandoning baseline data for a long time, was both utilized for outgoing longwave radiation data aiming at observing anomalies before and after six EQs. The findings show that the rise in data use discovered using the background field analysis approach was ambiguous. The occurrence time of anomalies was discrete and not continuous in the temporal distribution. The nonseismic and distant seismically associated fault structure areas had several longwave radiation improvement zones that significantly appeared in the spatial distribution.

IV. Overview of Data Communication Networks and Seismology

In this section, the dependence of seismology on modern communications methodologies is discussed. More specifically, we focus our discussion on the DCN which is considered a backend to the majority of communication systems. Accordingly, the DCN-involved elements are extensively clarified. On the one hand, as previously mentioned, seismology is the science of studying the EQ waves, the nonhomogeneity of earth structure, disaster management, and the EQ consequences mitigation. All of the mentioned aspects strictly need supporting technology to enhance the EQ parameters observation and detection. In addition, the flexibility of seismic data transmission from the seismic station to the observatories can be supported by such a technology. Moreover, the methodology of data gap retrieval can also be aided by modern technology.

Indeed, DCN is among the predominant technologies that can be effectively exploited to enhance the seismic wave detection process. Hereafter, the main DCN elements, protocols, media access techniques, and delays are briefly discussed as follows [29].

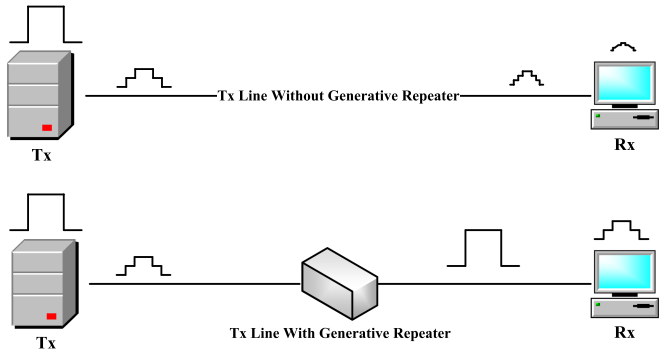

Fig. 4. Repeater effect.

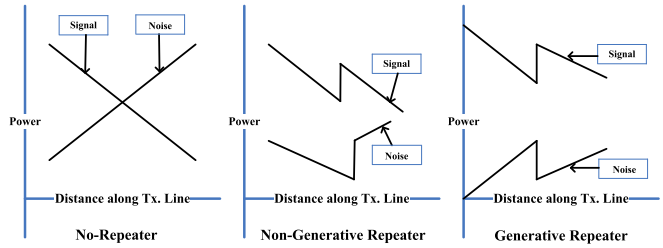

Fig. 5. Signal power with different repeater types.

A. Data Communication Network Elements

DCNs support many benefits over stand-alone computers. Throughout these elements, we can share terminology and common building blocks. The following sections briefly discuss the main DCN elements.

1) Client: The client is a computer/workstation within a network requesting the available resources from another computer on the network. The client can act as a server.

2) Server: The server is a managing computer on a network for the available shared resources, security, and applications in the network. Basically, the server has more processing capabilities and specifications than the client.

3) Workstation: The workstation is similar to a desktop or laptop, which could or could not be connected to a network. Mostly, clients are workstations.

4) Network Interface Card: The Network interface card is the internal electronic device inside a computer, which links a computer to communicate with other computers.

5) Backbone: The backbone is a part of a network. In other words, it can represent an interconnected part between a small part of a local area network (LAN) as shown in Fig. 8.

6) Repeater: The repeater is a device that fundamentally repeats the signal excluding the noise. It is classified into two types as shown in Fig. 4. The signal and noise power of the two repeater types are illustrated in Fig. 5. Because it costs more to provide synchronization signals between the transmitter and receiver, the generative repeater takes the data and retransmits it after one clock cycle. This results in high processing. The nongenerative repeater consists of an amplifier only, so it amplifies both the signal and the noise. This type of repeater is cheap.

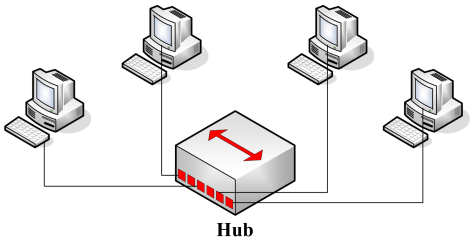

Fig. 6. Hub connection.

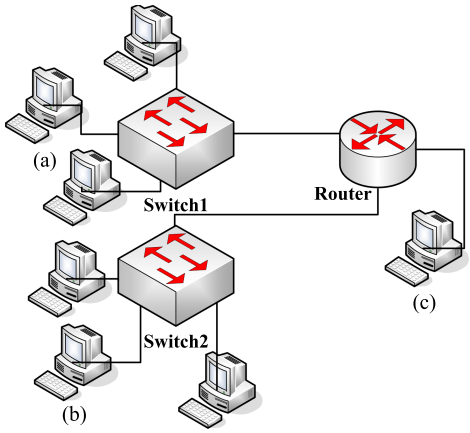

Fig. 7. Hub connection.

7) Hub: The hub is a layer one device, which means it can cope with line codings like Manchester and Differential Manchester since it understands layer one (physical layer), but not layer two (data link), hence it cannot grasp MAC addresses. It is also described as garbage in garbage out (GIGO). It makes the required cross-over and is considered as one collision domain because its connection is physically star but logically bus as shown in Fig. 6.

8) Switch: It is a layer two device that understands the data link layer (MAC address), and physical layer and it can perform broadcast for any received traffic. As an example, host (A) of Switch1 can connect to Host (B) directly, because each one of them is connected through layer two devices (switches) as shown in Fig. 7.

9) Bridge: The bridge is a layer two device. It understands the MAC address and reduces the number of collision domains as shown in Fig. 8.

10) Router: The router is a layer three (network layer) device, it can understand IP packets, MAC addresses, and bit streaming of the physical layer. The routers are used in a wide network or group of LANs to be connected by establishing routing tables containing all hosts' IPs in their LAN. Any host may discover the optimal route to the destination by using a variety of routers, as illustrated in Fig. 9 since the routers communicate information from these tables. The router interface to another network is called Gateway.

11) Topology: The topology is the layout of a computer network. It varies based on the network structure and the available hardware. The common types of network topologies are ring,

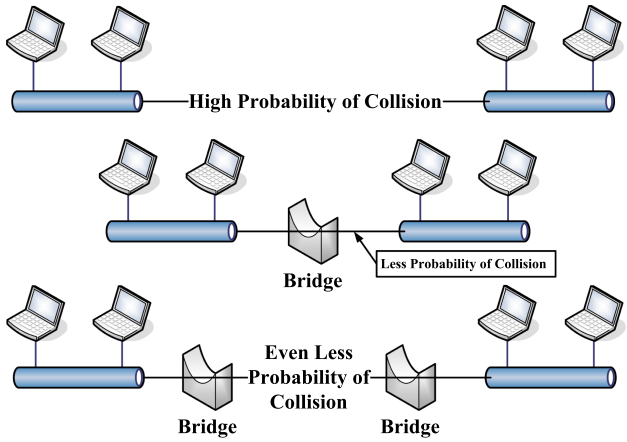

Fig. 8. Bridge connection.

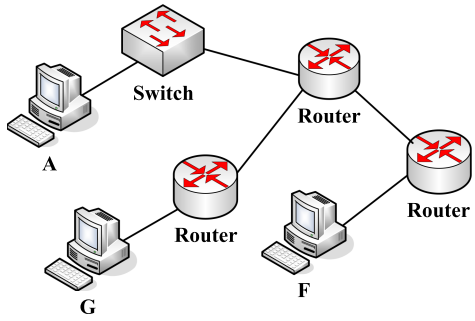

Fig. 9. Router connection.

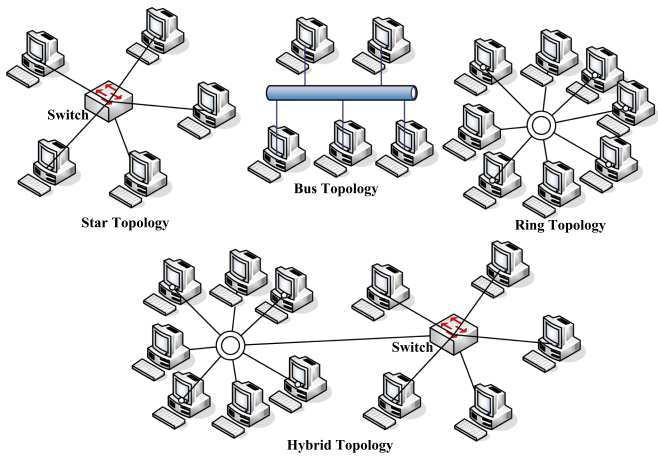

Fig. 10. Common network topologies.

star, bus, or hybrid combinations of them. Fig. 10 indicates these network topologies.

12) Transmission Media: It is the method of conveying data whether for transmission or receiving. Transmission media can be categorized as guided and unguided as illustrated in Fig. 11.

B. Transmission Reliability

To achieve reliable data transmission, the network needs some sort of overhead code, e.g., cyclic redundancy check (CRC), to

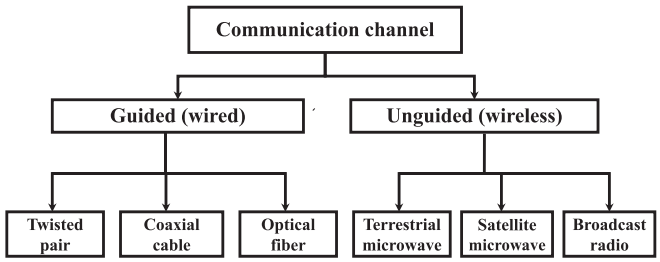

Fig. 11. Transmission media classification.

make sure the shack-hand transmission between the sender and receiver. In other words, an acknowledgment (ACK) can be used to assure that the transmitted packet has been correctly received and to pinpoint the lost packets. Once again, to effectively adapt a reliable data transmission, the following protocols can be employed.

1) Stop-and-Wait: This mechanism relies on an automatic repeat request scheme, which means that after transmitting a frame, the sender does not send the next frame till receiving an ACK about the last sent frame. This ACK adopts a timeout duration for receiving a such ACK. If the ACK is not received, the corresponding frame is considered lost and resent again. On the other hand, a potential problem can occur in which a duplicated copy of the same frame is delivered. To overcome such a problem, the header usually includes a 1-b sequence number (0 or 1) which is flipped for the next frame.

2) Sliding Window: In the process of the sliding window, the sender determines a sequence number (SeqNum) for each frame. Then, each one has a corresponding ACK but these ACKs are sent to the sender based on the truly received SeqNum frames. The sender adopts three variables: send window size (SWS) represents the upper limit of the number of ACK frames that can be transmitted, the last ACK received (LAR), and the number of the last frame sent (LFS) as formulated as in the following:

$$LFS - LAR \leq SWS. \tag{1}$$

On the other hand, the receiver addresses three variables: The receive window size (RWS), the largest acceptable frame (LAF); and the last frame received (LFR) as formulated in the following:

$$LAF - LFR \leq RWS. \tag{2}$$

C. Simple Demultiplexer (UDP)

The simplest transport protocol is the one that facilities the host-to-host service transmission of the underlying network. Due to the many processing capabilities desired, this protocol requires a level of demultiplexing to be able to serve the targeted applications. Indeed, a transport protocol via the Internet called user datagram protocol (UDP) is an example of a transport protocol.

It is well known that the involved mechanism to convert a website's Internet protocol (IP) to an applicable name is called domain name server (DNS). The UDP port multiplexing for several applications takes into consideration a message queue. It is worth mentioning that the UDP does not execute flow control or reliable delivery. It means that the sender is continuing packets transmission regardless the receiver is correctly receiving those packets. Accordingly, such a protocol is suitable for real-time applications.

D. Reliable Byte Stream/Transmission Control Protocol (TCP)

Due to the demultiplexing UDP protocol is not easy to implement and not guaranteeing message transmission reliability, another common protocol has been proposed called transmission control protocol (TCP). The TCP can guarantee transmission reliability where it relies on ACK hand-shake concept to assure that the message is correctly received. Besides, TCP is a full-duplex protocol that advocates a pair of byte streams. A byte is reserved for each direction. Moreover, the TCP supports a flow-control technique to manage the data stream transmission.

More particularly, the header is composed of some fields as each is responsible for a specific function in the transmission process. The SrcPort field determines the source port, while the DstPort field determines the destination port. Besides, these two fields, the source, and destination IPs are also involved. Then, The Acknowledgment, SequenceNum, and AdvertisedWindow fields are in charge of the sliding window technique. Afterward, the ACK and AdvertisedWindow fields convey information about the data flow moving in the opposite direction.

When the URG flag is forced, it means urgent data is needed to be processed. If the flag is activated, the UrgPtr field declares that the nonurgent data is now contained. The HdrLen field supports the header length (32-b). Finally, the Checksum field in TCP is the same as in the UDP. Moreover, it is applicable to measure when the packet transmission will start using the Offset field.

E. Routing Protocols

This section summarizes the routing protocols [30]. The routing protocols are summarized in Table III.

1) RIP: Routing information protocol (RIP) is one of the dynamic routing protocols. Its routing metric is the hop count to determine the best path between the sender and receiver. RIP is a distance-vector (DV) routing protocol. RIP employs port number 520.

2) IGRP: Interior gateway routing protocol (IGRP) is its DV routing protocol. IGRP controls the routing data flow within the communicating routers in the network. IGRP ensures the routing table attached to the connected routers that having the best path. IGRP is a loop-free routing protocol by continuous updating itself with the changes within the network.

3) EIGRP: Enhanced interior gateway routing protocol (EIGRP) is an advanced DV routing protocol. It is employed to adapt automating routing in computer networks. EIGRP is developed by Cisco Systems.

4) OSPF: Open shortest path first (OSPF) is an IP routing protocol. OSPF utilizes a link-state routing (LSR) mechanism, which is a member of the interior gateway protocols (IGPs) group.

5) IS-IS: Intermediate system to intermediate system (IS-IS) is a routing protocol for similar devices. IS-IS determines the

TABLE III
NETWORK PROTOCOLS COMPARISON

	RIP	IGRP	EIGRP	OSPF	IS-IS	BGP
Interior (In)/Exterior (Ex)	In	In	In	In	In	Ex
Algorithm (DV, HDV, LS, PV)	DV	DV	HDV	LS	LS	PV
Fundamental Metric	Hop count	Delay, BW, Reliability, and Load	Delay, bandwidth, reliability, and load	Cost	Cost	Multiple Attributes
Administrative Distance	120	100	90 In, 170 Ex	110	115	20 Ex, 200 In
Hop count Limit	15	255 (100 default)	224 (100 default)	None	None	EBGP Neighbors
Convergence	Slow	Slow	Very Fast	Fast	Fast	Average
Update timers	30 sec	90 sec	Only when change occurs (OWCO)	OWCO	OWCO	OWCO
Updates	Full table	Full table	Only Changes	Only Changes	Only Changes	Only Changes
Classless	Yes	No	Yes	Yes	Yes	Yes
Supports VLSM	Yes	No	Yes	Yes	Yes	Yes
Algorithm	Bellman-Ford	Bellman-Ford	DUAL	Dijkstra	Dijkstra	Best Path Algorithm
Update Address	224.0.0.9	224.0.0.10	224.0.0.10	224.0.0.5		Unicast
Protocol and Port		IP and 9	IP and 88	IP and 89		TCP and 179
Methodology	Routers based lowest hop count	Sends hello packets every 5s to neighbors checking the availability of neighbor	Sends hello packets every 5s to neighbors checking the availability of neighbor	Develops adjacencies with neighbors, periodically sending hello packets		Close to OFPS. Chose the best route.
Ideal topology	Chose networks less than 15 hops.	Any network, small to very large; Cisco routers only used.	Any network, small to very large; Cisco routers only used.	Any network, small to very large.	Any network, small to very large.	Used by ISPs & Large Enterprises.
Standard	RFC 1388	Cisco	Cisco	RFC 2328	RFC 1195, 5304	RFC 1105
Strengths	Easy to configure and use.	Easy to configure and use. Delay, BW, reliability, and link load are the metric.	Utilizes DUAL for very quick converge and a loop-free network. Advocates IP and IPX.	Converges quickly. Routing update packets are small. Not prone to routing loops.		
Weaknesses	No. Hop is 15; Converge slowly No info about BW No multipath	Not Internet std.; Only use Cisco routers Converges slowly than RIP.	Not an Internet standard; all routers must be from Cisco Systems.	More complex to configure and understand than a distance vector protocol		

best path for moving the data based on the packet-switched concept.

6) BGP: Border gateway protocol (BGP) is a standardized ExGP for information reachability on communicating devices via the Internet. The BGP is a path vector (PV) but sometimes is considered a DV protocol.

F. Delays

The data network performance depends on two main parameters, which are delay and utilization. Let us start by delay; it can be classified as follows.

1) TX. delay: The amount of time used until the last bit departs the transmitter.
2) Propagation delay: The amount of time needed for data to be sent between the transmitter and receiver.
3) Queuing delay: The receiver buffer is filled with data that has to be processed at the produced time.
4) Processing delay: The amount of time used to process particular data.
5) Reassembly delay: The amount of time needed to reconstruct data that was previously assembled at a transmitter.

Continued improvement in the optimizing algorithms on which the network depends and improved performance of routers in particular (i.e., speed of decision-making and reduced propagation delay) have resulted in reduced data transmission times. By coupling the reduced transmission times with a greatly reduced total cost, more people can use the Internet and data networks in general. Despite the increase in users, the performance of the network has not generally degraded (except on the odd occasion when the system is overloaded).

G. Media Access Techniques

The secondary data network performance parameter is the utilization relying on media access techniques. These techniques can be classified as follows.

1) Round Robin: Round Robin checks finding data at subscribers to be sent as shown in Fig. 12, where it is similar to the token of the ring topology. This technique mainly depends on the central controller that surveys which subscriber needs to

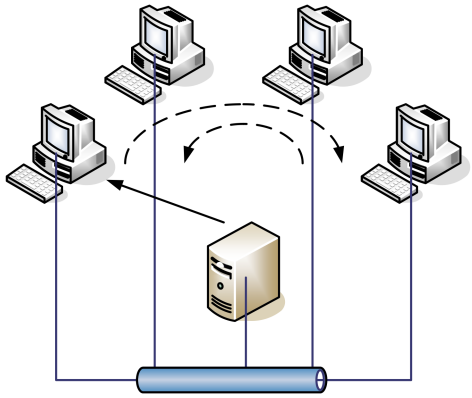

Fig. 12. Round robin operation.

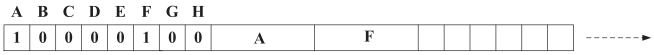

Fig. 13. Controller technique of reservation media access technique.

send. But the potential problem with which subscriber needs to send.

2) Reservation: a) *Controller:* This system solved the Round Robin problem by using dedicated time slots for each subscriber and reserving all time where each subscriber is represented by one bit inside the frame that comes before the transmitted data called reservation slots.

This data are sent according to the ranking of the bit's subscriber, where the subscriber data are available depending on the corresponding bit. If the incoming "1" means that its subscriber will send and vice versa as shown in Fig. 13. But the problem of this system is concentrated in the utilization because the channel is always reserved even when no needed data is sent. Note that only subscribers A & F will send and the reservation slots = 8.

b) *Request to send:* This system uses a contention period like a reservation frame or reservation request for each subscriber before sending data. This period is very small, whereas if a certain subscriber sends a contention period during another it does not cause a large influence.

3) Contention: Contention can be illustrated in Fig. 14 as it represents three subscribers; each one sends at least two packets. Indeed, contention has four submechanisms as follows:

1) ALOHA;
2) slotted ALOHA;
3) carrier sense multiple access (CSMA);
4) carrier sense multiple access with collision detection (CSMA/CD).

The different access techniques' utilizations are calculated for the following example of as the following. ALOHA utilization = 3/11= 27%, slotted ALOHA utilization = 4/11 = 36%, CSMA utilization = 7/11 = 63% and CSMA/CD utilization = 7/11 = 63% as shown in Fig. 14. Note the difference between CSMA and CSMA/CD. CSMA/CD avoids the collision by sensing the channel all the time before and after sending, but CSMA only senses before sending.

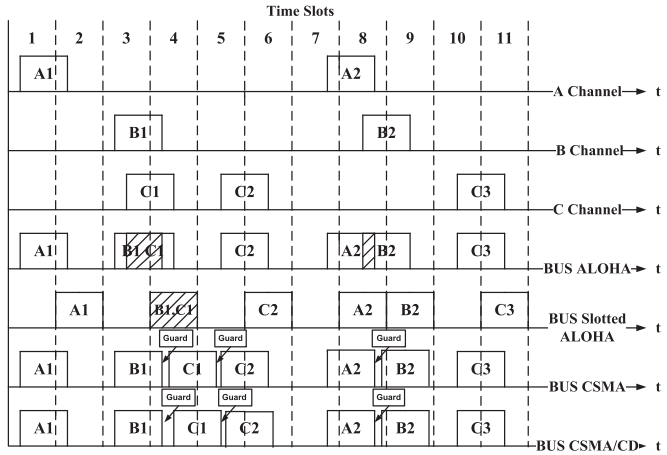

Fig. 14. Media access technique utilizations.

H. Transmission of Real-Time Monitoring Data

All of the seismic stations are connected to the processing center by a dedicated telecommunication technique. The data center needs to receive all of the station's crucial information. Disasters might, however, devastate the crucial network infrastructure needed to connect to the data center. Therefore, relying solely on one type of communication backhaul may be too dangerous. Different forms of backhaul may be used in an emergency communication network to boost robustness.

In Table IV, each group of communication network techniques is compared in terms of application coverage, emergency survival, ability to self-organize when network infrastructure is partially damaged, deployment cost, deployment time, and whether preexisting infrastructure exists.

V. Data Communication-Based Advanced Networks for Seismology

In this section, the supporting advanced networks for seismology that rely on the data communication traffic and communications concepts are studied.

A. Acoustic Sensors for Seismology

Recently, distributed acoustic sensing (DAS) methodologies have fast booming for representing the dense seismic array using fiber-optic cables. This methodology is cost-effective. The DAS is employed for time-lapse imaging for the velocity of the shear wave. This mechanism is based on an integration of the surface waves multichannel analysis and the ambient noise interferometry [31]. In [31], the authors have built that imaging by utilizing a linear DAS array to record the traffic noise for three continuous weeks. The authors have observed subtle changes near the surface such as water content variations.

B. Social Networks for Seismology

Nowadays, the power of social networks has become an intrinsic tool and supports the decision-maker. More concretely,

TABLE IV
COMPARISON BETWEEN DIFFERENT GROUPS OF EMERGENCY COMMUNICATION NETWORK TECHNOLOGIES

Technology	Coverage	Selforganizing	Survivability	Cost	Delay	Existed
WiFi	Wide	Good	Low	Low	Low	Yes
Wired	Wide	Not good	Low	Moderate	Low	Yes
P2P	Not wide	Good	Low	Low	Low	Yes
Cellular Network	Wide	Good	High	Low	Low	Yes
Satellite	Wide	Good	Extremely high	Extremely expensive	High	Yes

TABLE V
EQS VERSUS TWEETS

Location	Hokkaido, Japan	Lombok, Indonesia
Date and Time	05/09/2018 and 18:07:58 UTC	05/08/2018 and 11:46:37 UTC
Magnitude	6.6	6.9
Effects	41 killed and 680 injured	563 killed, 7,000+ injured, and 431,436 displaced
Analyzed Tweets	117,810	92,185
Original Tweets	30,487(26%)	23,211(25%)
Retweets	83,686(71%)	67,159(73%)
Replies	3,637(3%)	1,815(2%)
% English Tweets	66%	75%

it can be employed to preserve human lives during natural disasters. In [32], the authors advocated employing all-encompassing solutions that use the power of social media to lessen the harmful effects. The role of social media has been also exploited in [33]. More particularly, it can be employed to support dominated data about the infrastructure status. Moreover, social media can be utilized as a disaster indicator.

In [33], the authors noticed an anomaly in Twitter activity to specific EQs that occurred in 2018. Accordingly, they selected the dominant EQs, and then, categorized these EQs into certain patterns to analyze the users' activities during them. The authors have estimated a correlation between the Twitter's activity and those patterns as more than four million tweets have been published during the EQs' times. Moreover, it was estimated that Twitter's activity is directly proportional to the EQ magnitude. However, the authors have ensured that the main parameter is the intensity of EQ along with the density of the population.

The authors in [34], have considered the first feedback and relief administrations. Another point of view has been adopted in which the message transmission can be utilized in the warning phase [35]. Another study has elected social media for improving the awareness of handling the emergency situation [36]. Social media has been also extended to be used for real-time monitoring of natural disaster [37]. The role did not stop here, the United States Geological Survey had investigated the short text message to enhance the gathered information for hazard assessment [38]. Table V indicates the characteristics of dependence on EQ and social media throughout two events.

C. Internet of Things Networks for Seismology

To mitigate the effects of a natural disaster that might worsen human life, EEW has become crucial. For EQ mitigation, a lot of research has been done using the satellite system, IoT, 5G, RFID, software-defined network (SDN), network functions virtualization, DCNs, and other technologies [39], [40], [41], [42]. Additionally, social media played a minor effect in EQ catastrophe risk reduction. In [32], the authors offered a perspective on adopting all-encompassing solutions that combined the strength of social media with cutting-edge networks to mitigate the negative effects.

The literary context's efforts expanded beyond the use of remote sensing, which was backed by satellite observation [43], but also included the use of software-defined networks and network function virtualization, which incorporated IoT on-the-fly gateways [44]. The goal of the endeavor was to assist the large-scale domains whose infrastructures had been destroyed in whole or in part. The reorientation of catastrophe risk reduction can potentially benefit from virtualization. According to [45], a catastrophic scenario portraying an early warning system for a safe evacuation from catastrophe risks was portrayed by integrating the cloud system and the heterogeneous virtual network.

All of these initiatives are put forth alongside the conventional approaches to EQ detection, research, and fault rupture type distinction, all of which have received substantial study in the literature (see, for example, [46] and [47]. According to [48], the authors suggested a local similarity EQ detection approach that relied on the idea of the nearest neighbor methodology to assess the received signal coherence between the targeted stations and their closest neighbors. Other investigations concentrated on EQ magnitude estimates using the first few seconds as a substitute for the whole rupture [4], [48], [49].

The time restriction still requires additional work and research, though, as it takes a while to compute the EQ parameters using conventional methods. It is interesting that regardless of the chosen strategy, there is typically a waiting period until the source time function develops sufficiently. The actual computation time, however, might vary from one scheme to another. Due to the dependence between the monitored window width and the blind zone size, the initial few seconds are crucial for EEW. In that time frame, it is possible to assess the P-arrival wave's timing and magnitude, which is the first incoming EQ wave. It is important to note that the wider the blind zone must be taken into account for the required reservation before the arrival of the powerful EQ waves, the longer the assessed window size.

According to [50], a data-driven core type from an EWS has been proposed for ecological catastrophe risk management utilizing an IoT system. The writers of [51] and [52] have talked about how to stop a disaster from spreading by effectively exchanging information across many platforms and

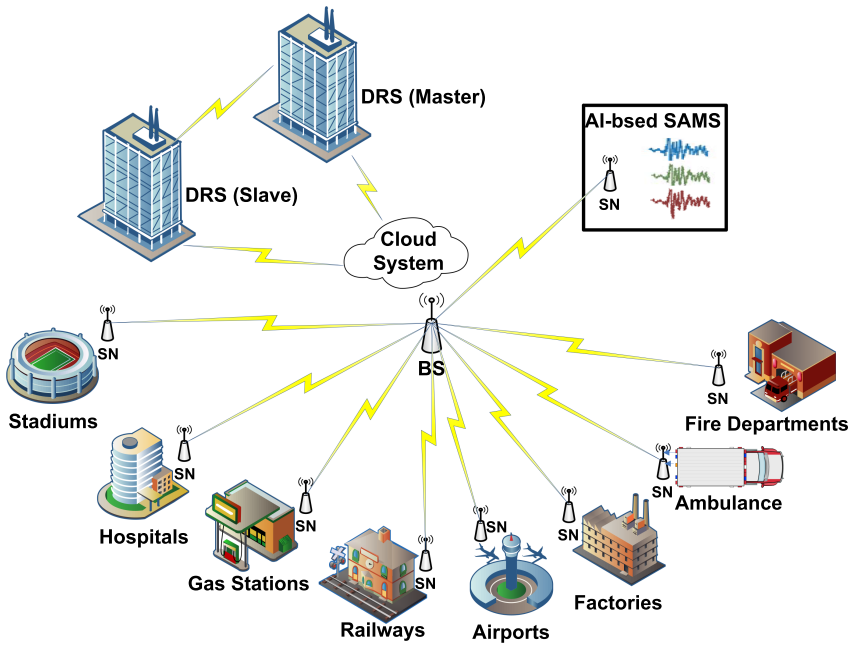

Fig. 15. General architecture of IoT system-based EEW.

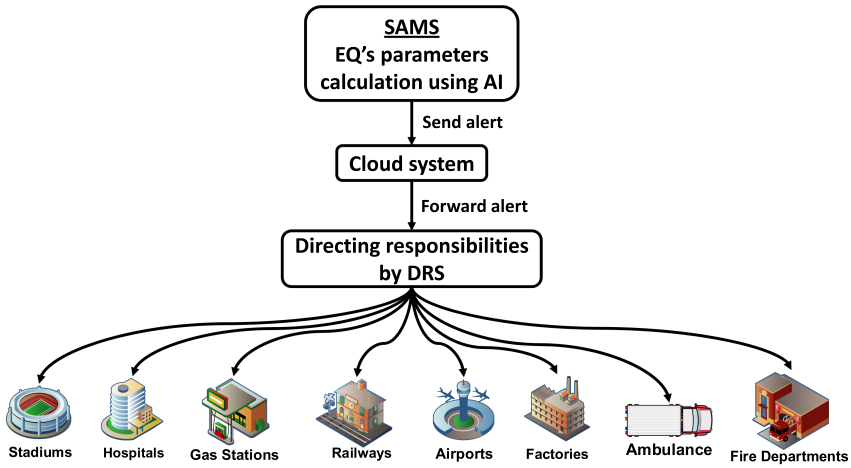

Fig. 16. Work flow of the general system.

utilizing IoT/M2M/D2D connectivity for adaptable data flow. Additionally, the EEW [53] has taken use of the message queuing telemetry conveyance and the sensor web application.

The authors of [3] described an IoT-based EEW system, as seen in Fig. 15. It is important to note that the seismic activity monitoring and analysis system (SAMS), which is a real-time program, uses artificial intelligence. The AI algorithms will automatically assess the earthquake activity. The suggested process is shown in Fig. 16 starting with the alert trigger based on the EQ's characteristics and continuing until the appropriate action is taken in the EQ catastrophe risk mitigation by the relevant organization.

More specifically, communication between the SAMS system and other IoT elements will take place over a base station that is attached to the IoT cloud. To be more specific, as soon as the SAMS system recognizes the parameters of an upcoming EQ, SAMS will immediately transmit an alarm message—which includes the EQ parameter—-to the disaster recovery system (DRS) via the IoT cloud.

In response, the DRS will determine the necessary actions to be done and promptly connect with all IoT system parts through the IoT cloud. In this scenario, the DRS is viewed as the central unit that determines the actions that must be taken by each entity in the IoT system, including ambulances, hospitals, fire departments, airports, railways, gas stations, stadiums, and factories, to quickly take the appropriate action, such as rescuing, evacuation, etc., to lessen the effects of the EQ disaster.

The DRS then notifies each entity of the activities that need to be taken. More specifically, by utilizing the SNs, every component of this system may be notified of the required action

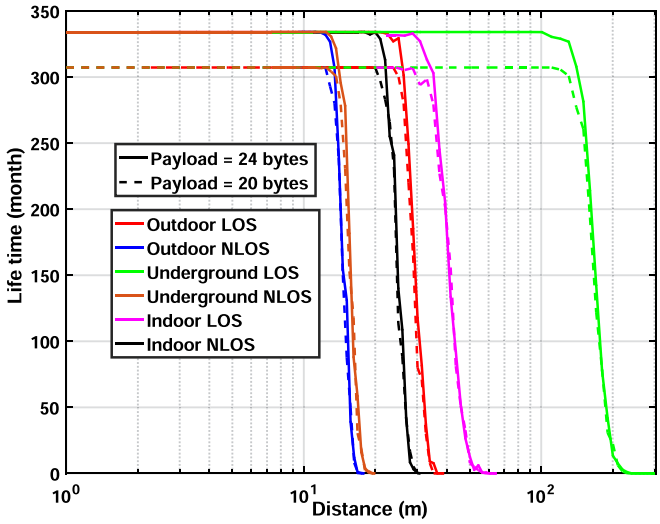

Fig. 17. Lifetime statistics versus the internode distance for IoT SN.

triggered by the cloud (SNs). These systems ought to take advantage of the SNs connected to IoT devices. Tmote Sky SN is one of these SN kinds that is frequently used in IoT networks using the IEEE 802.15.4 standard, boosting accurate locations, and various sizes for IoT. Additionally, as thoroughly researched in [54], it may function well in a variety of contexts where security vulnerabilities are present [55], [56].

In the trajectory of implementing IoT systems for EEW, the authors in [3] studied the data on the lifespan of IoT SNs based on the IoT network. In this study, the Tmote Sky SN has been adopted, which is frequently used in IoT applications. This study considered the extensive work presented in [57]. The study investigated the lifespan of the Tmote Sky SN in six distinct environments: outside LOS, outdoor NLOS, subterranean LOS, underground NLOS, interior LOS, and inside NLOS. More particularly, the specifications of maximizing the lifetime are discussed. In the six scenarios investigated, the authors demonstrated the IoT SNs' lifespan outcomes when the payload size is either 24 or 20 B.

In this regard, the adopted study in [3] presented by Fig. 17 shows the network lifespan as a function of inter-node distance for a network of sixteen SNs in the six settings used. Regarding the environments of the outdoor line of sight (LOS), outdoor nonline of sight (NLOS), subterranean LOS, underground NLOS, indoor LOS, and indoor NLOS, the network lifespan will be fixed at 334.1 months for internode lengths of 20, 11.2, 90.7, 12.4, 28.73, and 18 m with a payload length of 24 B. When the same six environments are used, the network lifespan is set at 307.2 months for internode lengths of 23.8, 11.77, 110.6, 12.4, 24.47, and 19 m with a payload length of 20 B. It should be noticed that as the payload length grows, the internode distance shrinks. As a result of the environmental difficulties, the likelihood of retransmitting packets is reduced, and therefore the packet overhead is minimized. As a result, as the payload length grows, so does the network lifespan. The collected six environments' findings are summarized in Table VI.

TABLE VI
LIFETIME OF IOT NETWORK COMPOSED OF WHERE PAYLOAD LENGTH $\in \{20, 24\}$ BYTES OVER THE SIX ENVIRONMENTS

Environment	Payload length			
	24		20	
	T_l (month)	D(m)	T_l (month)	D(m)
Outdoor LOS	334.1	20	307.2	23.8
Outdoor NLOS	334.1	11.2	307.2	11.77
Underground LOS	334.1	90.7	307.2	110.6
Underground NLOS	334.1	12.4	307.2	12.4
Indoor LOS	334.1	28.73	307.2	24.47
Indoor NLOS	334.1	18	307.2	19

VI. OPTIMIZATION AND SEISMOLOGY

Basically, optimization is achieving the maximum benefit with the minimum cost. More particularly, any problem is represented by a mathematical formula. The formula is called the objective function. The function is restricted by some constraints that determine the space of search to the optimization problem to investigate the optimal solution.

In this section, the role of optimization for seismology. Two pivots are included. First, optimization is employed to handle the seismic signals for a more flexible inversion. Second, the seismic network has some weaknesses in preserving the network lifetime, optimizing the packet size, and reducing the power consumption.

A. Optimization and Seismic Signals

This section extensively discusses the state-of-the-art concerning optimization techniques for seismic signals. Generally speaking, inversion is one of the main benefits of utilizing optimization for seismology. In the field of oil-and-gas exploration, seismic inversion can play a significant role in representing the reflection of seismic data to a quantitative rock property. In other words, the seismic inversion is an effective representation of bulk density and sonic velocity.

In [149], a multiobjective function has been used for seismology. Three broadband datasets have been used. The first seismic dataset is acquainted with a network in the Middle East. The second dataset is truncated from Texas Gulf Coastal Plain. The third one is related to SE New Mexico and West Texas. In [150], the authors analyzed convergence and stability using a specific branch of optimization called differential semblance optimization to estimate reflection seismology. This approach explores changes in the resulting least-square-inversion in seismograms and their numerical properties. More particularly, that model studied the conventional approximation inversion of the plane-wave seismograms throughout an acoustic media of layered-constant density.

In [151], a particle swarm optimization (PSO) model has been proposed to calculate the peak ground acceleration (PGA). PGA is among the main parameters pinpointing the EQ intensity. The model was developed to estimate the PGA based on the Iraqi database. More specifically, the authors relied on 187 historical records of ground motion of Iraq's tectonic regions.

TABLE VII
CLASSIFICATION OF OPTIMIZATION TECHNIQUES IN SEISMOLOGY

Classical	Newton's theorem [58], [59], [60], [61], [62], [63], [64], [65], [66]		Secant theorem [67], [68], [69], [70], [71],		Lagrange multiplier [72], [73], [74], [75], [76], [77], [78]		
Numerical	Linear programming [79], [80], [81], [82], [83], [84], [85]	Integer programming [86], [87], [88], [89], [90], [57], [91], [92]	Quadratic programming [93], [94], [95], [96], [97], [98], [99], [100], [101]	Non-linear programming [102], [103], [104], [105], [106], [107]	Stochastic programming [108], [109], [110], [111], [112]	Dynamic programming [113], [114], [115], [116], [117], [118]	Combinatorial [119], [120], [121], [77], [122], [123]
Advanced	Genetic algorithm (GA) [124], [125], [126], [127], [128], [129], [130]		Particle swarm [131], [132], [133], [134], [135]	Karush–Kuhn–Tucker (KKT) [136], [137], [138]		Simulated annealing [139], [140], [141] [142]	Ant colony [143], [144], [145], [146], [147], [148]

That model has considered certain seismic parameters such as average shear-wave velocity, EQ magnitude (Mw), focal depth, and nearest event location to a seismic station. In [152], an optimization function has been developed as an inversion for exploring heterogeneous geological layers. Using optimization has been extended to be used for seismological modeling. In [131], the authors proposed a multiobjective PSO based on Pareto for seismology modeling. Table VII categorizes the different optimization techniques for seismic signals analysis. Optimization can also contribute to accurate data observation and management [3], [57], [153], [154], [155], [156], [157], [158], [159], [160], [161].

B. Optimization for Prolonging Seismic Network Lifetime

Optimization is among the desired advanced techniques that are utilized to prolong the network's lifetime. It is well known that the seismic network is among the most vulnerable networks that strictly need to keep its resources as long as possible. This is because of being the seismic network is mostly located at very far locations. In this section, the importance of optimization is discussed. More particularly, mixed integer programming is extensively employed for prolonging the network lifetime and optimizing the nodes' interdistance.

On this front, the path loss model between the communicating nodes i and j can be given by

$$PL_{ij}\,\mathrm{dB} = PL_0\,\mathrm{dB} + 10n\log_{10}\frac{d_{ij}}{d_0} + \sigma[\mathrm{dB}] \tag{3}$$

where PL_0 denotes the free space path loss with the reference distance d_0 of the antenna far-field, n is the path loss exponent, d_{ij} is the distance between the sending node i and the receiving node j, and σ represents the shadow fading standard deviation in dB.

The signal power of the received antenna based on a power level m can be derived as

$$P^A_{r,ij}(m)[\mathrm{dbm}] = \mathrm{P}^{\mathrm{A}}_t(m)[\mathrm{dBm}] - PL_{ij}[\,\mathrm{dB}] \tag{4}$$

where $P^A_{r,ij}(m)$ denotes the signal power of the transmission antenna with power level m. The transmission power usage with eight power levels that is accessible (P_{ct}) and the antenna transmission power (P^A_t) along with the corresponding power level relying on the Tmote Sky node [162] are listed in Table VIII.

TABLE VIII
TRANSMISSION POWER VERSUS POWER LEVEL

P_{ct}	P^A_t	m
25.5	-25	3
41.7	-5	19
29.7	-15	7
45.6	-3	23
33.6	-10	11
49.5	-1	27
37.5	-7	15
52.2	0	31

TABLE IX
PATH LOSS PARAMETERS

Environment	n	σ	$P_n(\mathrm{dBm})$
Outdoor LOS	2.42	3.12	-93
Outdoor NLOS	3.51	2.95	-93
Underground LOS	1.45	2.45	-92
Underground NLOS	3.15	3.19	-92
Indoor LOS	1.64	3.29	-88
Indoor NLOS	2.38	2.25	-88

The SNR between the transmitting node and the receiving node is derived by

$$\gamma_{ij}(m)[\mathrm{dB}] = P^A_{r,ij}(m)[\mathrm{dBm}] - P_n[\mathrm{dBm}] \tag{5}$$

where P_n represents the noise power at the receiver. Table IX indicates the path loss parameters within the available six environments that are measured by [163].

Indeed, when quadrature phase shift keying (O-QPSK)-based offset is adopted the probability of error (BER) is denoted by

$$BER = Q\left(\sqrt{\frac{2E_b}{N_0}}\right) \tag{6}$$

where $\frac{E_b}{N_0}$ is derived as

$$\frac{E_b}{N_0} = \gamma_{ij}(m)P_{rG} \tag{7}$$

where P_{rG} is the process gain.

The probability of a correctly received packet of L-Byte packet transmitted at m power level of the communicating nodes

TABLE X
SUMMARY OF AI ROLE IN SEISMOLOGY

Model target	Model type	Performance achievement	Supervised (S)/ Unsupervised (US)	Ref.
Denoising	DeepDenoiser (AE)	Acc $\rightarrow$ 85.8%–98.9%, Exceed MAE with 2.38×10^{-5}	S	[164], [165]
	DNN	Based on SNR	US	[166]
	DeepTensorCNN	Based on SNR	S	[167]
	Dual-path RNN	Via scale-invariant SDR & SNR	S	[168]
Clustering	AP	SDR, and SNR	S	[169]
	DCAE	Acc $\rightarrow$ 91% - 98.5%	US	[170]
	HSVR	Hierarchical	S	[171]
	Deep scattering network	Hierarchical	US	[172]
Location	DAE with CNN	MSE $\rightarrow$ 0.0000515	S	[3]
	CNN	Acc $\rightarrow$ 74.6%	S	[173]
	DCNN	Location error $< 300m$	S	[174]
	LSTM-FCN	Acc $\rightarrow$ 89.1%	S	[175]
Magnitude	DAE with CNN	MSE $\rightarrow$ 0.000028	S	[3]
	CNN and RNN	MSE ≈ 0 and SD ≈ 0.2	S	[176]
	SVM	SD ≈ 0.33	S	[177]
Phase detection	CNN	Acc $\rightarrow$ 99.8%	S	[178]
	CNN with RNN	Acc $>$ 98%	S	[179]
	PhaseNet software	Acc $\rightarrow$ 50% - 60%	-	[180]
Picking	CNN	Acc $\rightarrow$ 63.8%	S	[181]
	CNN	Acc $\rightarrow$ 92.5% - 98.6%	S	[182]
	CNN	Acc $\rightarrow$ 95%	S	[183]
	Capsule network	Acc $\rightarrow$ 97.64	S	[184]
	CNN with RNN	Acc $>$ 98%	S	[179]
	LSTM	Acc $\rightarrow$ 98.8%	S	[185]
PPV	ANN	Acc $\rightarrow$ 95%-98.6%	S	[186], [187]
	SVM	Acc $\rightarrow$ 96%-99%	S	[188], [189]
	FIS	Acc $\rightarrow$ 95%	S	[190]
	ANFIS	Acc $\rightarrow$ 98%	S	[191]
	DT	Acc $\rightarrow$ 99.7%	S	[192]
Seismic acceleration	US manifold-approximation	-	US	[193]
	ensemble SWARA-ANFIS-PSO	ROC $\rightarrow$ 89.4% - 93.6%	S	[194]
	Gradient boosting	R2	S	[195]
Quarry-blast and EQ classification	ANFIS-GWO	Acc $\rightarrow$ 99.8%-99.9%	S	[196]
	CNN and RNN	Acc $\rightarrow$ 99%	S	[197]
	ANN	Acc $\rightarrow$ 89%	S	[198]
	Manifold learning techniques	Acc $\rightarrow$ 94.44%-99.05%	S	[199]
Estimating incomplete regular and irregular data	CNNs	-	S	[200]
	Encoder-decoder-style U-net CNN	Acc $\rightarrow$ 71.7% - 99.7%	S	[201]
EWS parameters	DAE with CNN	MSE $\rightarrow$ .0001 - 0.0000033	S	[3]
	LSTM	Missed alarm rate of 0% and a false alarm rate of 2.01%	S	[202]
	CNN	Error in location 8.5–4.7 km	S	[203]
	Ncheck algorithm and Multitarget regression	MAE in origin time is 2.78 s, MAE in location is 27.81	S	[204]
Landslide	U-Net	Acc (Mean intersection over union (MIoU)) $\rightarrow$ 88.4%, 84.17%	S	[205], [25]
	Adaptive sampling and random forest	Acc (AUC) $\rightarrow$ 90.6%	US	[206]
	CNN with Random forest	Acc (AUC) $\rightarrow$ 95%	S	[207]
	Deep CNN	Acc $\rightarrow$ 95.05%, 99.42%, 81.17%, MIoU $\rightarrow$ 56%	S	[208], [209], [210], [211]
	AE	Acc (F1) $\rightarrow$ 74.9%-89.1%	US	[212]
	LandsNet	Acc $\rightarrow$ 86.89%	S	[213]
	Full convolutional network	Acc $\rightarrow$ 88.2% - 93.85%	S	[214]
	Random forest	Acc $\rightarrow$ 93.2%	S	[215]
	SVM	Acc $\rightarrow$ 80% - 94%	S	[216]

i and j is denoted by

$$p_{ij}^{S}(m, L) = \left(1 - Q\left(\sqrt{16\gamma_{ij}(m)}\right)\right)^{8L}. \quad (8)$$

Conversely, the probability of failure to receive a packet is

$$p_{ij}^{F}(m, L) = 1 - p_{ij}^{S}(m, L). \quad (9)$$

Accordingly, the successful hand-shake in which the packet is correctly transmitted with a probability p_{ij}^{S} with a power level m and an ACK is already transmitted to the sender at power level u with a probability p_{ji}^{S} is given by

$$p_{ij}^{SHS}(m, u) = p_{ij}^{S}(m, Z_k) \times p_{ij}^{S}(u, Z_{ACK}). \quad (10)$$

TABLE XI
CLUSTERING ALGORITHMS COMPARISON

	DBSCAN	HDBSAN	K-means	Agglomerative	AP
Clustering based	Density and distance	Density and distance	Kernel	Hierarchy	Graph
Pros	- Appropriate for data of any form	- Appropriate for data of any form - Appropriate for high dimensional feature space	- Appropriate for data of any form - Appropriate for high dimensional feature space - Able to evaluate noise and find overlapping clusters	- Appropriate for data of any form - The hierarchical link between clusters is simple to identify.	- Simple and obvious - Disregard for the extremes - Beforehand, the number of clusters is not wanted.
Cons	- Poor quality and uneven data space density - Clustering is very dependent on the variables	- Poor quality and uneven data space density - Clustering is very dependent on the variables - Not noise-resistant - Impacts of chaining have an impact	- Unfit for handling massive amounts of data - Clustering is very dependent on the variables - High complexity at the beginning	- A lengthy complexity - Prior planning is required for number of clusters.	- A lengthy complexity - Clustering is very dependent on the variables
Algorithm Complexity	$O(NlogN)$	$O(N^2)$	$O(iCN)$	$O(N^3)$	$O(N^2logN)$
Keynotes	N is the number of objects, C is the number of clusters, and i is the number of iterations.				

Therefore, the failure hand-shake probability is derived by

$$p_{ij}^{FHS}(m,u) = 1 - p_{ij}^{SHS}(m,u). \tag{11}$$

Afterward, the retransmission number to make sure the packet is correctly received is given by

$$R_{e_{ij}}(m,u) = \frac{1}{p_{ij}^{SHS}(m,u)}. \tag{12}$$

To calculate the required energy for transmitting (Z_k)-byte packet from a node i to node j at a power level m, the following formula is adopted:

$$E_{dt}\left(m, Z_k\right) = P_{ct}(m) T_t Z_k \tag{13}$$

where T_t is the transmission time. The total energy consumption is

$$E_t^{HS}\left(m, Z_k\right) = E_{dt}\left(m, Z_k\right) + P_{cr}\left(T_s - T_t\left(Z_k\right)\right) \tag{14}$$

where T_s is the duration of the time slot, T_t is the real transmission time, while P_{cr} is the power consumption in the rest of the slot.

The energy consumption in the packet retransmission till achieving a successful handshake is given by

$$E_{dt}\left(m, Z_k\right) = E_{dpp} + R_{e_{ij}}(m,u) E_t^{HS}\left(m, Z_k\right) \tag{15}$$

where E_{dpp} is the energy dissipated in packet processing till attaining a successful hand-shake. On the other hand, the successful hand-shake at the receiver is given by

$$E_r^{SHS}\left(u, Z_k\right) = P_{cr}\left(T_s - T_t\left(Z_k\right)\right) + E_t^{ACK}\left(u, Z_k\right). \tag{16}$$

On the other hand, the energy consumed when a failure hand-shake occur is given by

$$E_r^{FHS}\left(u, Z_k\right) = P_{cr} T_s. \tag{17}$$

Similarly, the total energy consumed at the receiver side including the retransmissions and their ACKs is derived by

$$\begin{aligned} E_{r,ji}^{SHS}&\left(u, Z_k\right) \\ &= E_{dpp} + R_{e_{ij}}(m,u)\left\{P_{ij}^{SHS}(m,u) \times E_r^{SHS}\left(u, Z_k\right)\right. \\ &\quad + p_{ij}^{S}\left(m, Z_k\right) \times P_{ji}^{F}\left(u, Z_{ACK}\right) E_r^{SHS}\left(u, Z_{ACK}\right) \\ &\quad \left. + p_{ij}^{F}\left(m, Z_k\right) E_r^{FHS}\right\}. \end{aligned} \tag{18}$$

Therefore, the generated data packets represent the difference between incoming packets and outgoing packets is given by

$$N_r G_i^k = \sum_{(i,j)\in y} k_{ij} - \sum_{(j,i)\in y} k_{ji} \quad \forall i \in X \tag{19}$$

where G_i^k is the generated packets by the node i per round, N_r is the number of iterations, y is the set of possible pairs of nodes, and X is the set of nodes regardless the base-station. To calculate the total busy time for any node i, the following formula is utilized:

$$\begin{aligned} T_b = T_s &\left\{ \sum_{(i,j)\in y} R_{e_{ij}(m,u)} k_{ij} + \sum_{(j,i)\in y} R_{e_{ji}(m,u)} k_{ji} \right\} \\ &+ N_r T_A, \forall i \in X \end{aligned} \tag{20}$$

where T_A is the data acquisition time, k_{ij} denotes the packets transmitted from node i to node j. Conversely, k_{ji} expresses the packets transmitted from node j to node i.

VII. ARTIFICIAL INTELLIGENCE AND SEISMOLOGY

Recently, AI has played a revolutionary role in seismology, by which the stack holder can understand more about the complex earth structure. Accordingly, many phenomena can be interpreted and more reliable solutions can be presented for

saving human life. In other words, strategic risk reduction maps and threat mitigation can be attained. In this regard, here we aim to evaluate the crucial role that AI can contribute. More particularly, we focus on the main methodologies contributing to seismology, such as fuzzy logic, machine learning (ML), and deep learning (DL).

More information on ML and DL is included in the discussion that follows. Intriguingly, DL is one of the contemporary technologies that contribute significantly to the resolution of complicated issues without a specific mathematical method [216], [217], [218]. DL is a preeminent technique for both regular and irregular data mining and reconstruction. A DL model has been suggested in [200] and [219] to estimate the partial regular and irregular seismic data. The performance of the model was evaluated using the mean-squared-error loss function and was then optimized using the Adam method [220].

Table X addresses the common studies that employed AI in different ways for seismology. More concretely, the table presents a taxonomy of utilizing both ML and DL for specific targets in seismology, i.e., denoising seismic waves, seismic area clustering based on seismicity level, and determination of the EQs' location, magnitude, phase, and picking. Moreover, this taxonomy presents the role of AI in predicting the peak particle velocity (PPV), which is essential for saving the environment against the abnormal activities of the quarry blasts, besides, detecting the seismic wave acceleration and determining the PGA. The table also summarizes the main efforts exerted for classifying the EQs and quarry blasts, estimating the incomplete regular and irregular seismic data, and finally calculating the desired parameters for achieving successful EEWS. Indeed, the clustering of seismicity levels is among the main hazardous issues facing the stack holder. Therefore, we list an individual classification for the clustering algorithms types affected by AI based on their advantages and disadvantages as presented in Table XI.

VIII. Conclusion

EQ is among the most catastrophic natural disasters that need a reliable, intelligent, and integrated solution. Although many research efforts have been presented in the literature context, such a phenomenon still requires a prominent solution. Such a solution can alleviate risk to human life, meet the day-to-day challenges, and handle the vulnerabilities of the vital places against the EQ disaster. Accordingly, the efficient employment of the fast booming technologies and techniques can be a pivot toward a robust EEWS. The article denotes the essential roles that can be played by communication systems, optimization, IoT, AI, and social media in the different fronts of seismology aiming at achieving autonomous EEWS. First, the need for modern technologies for seismology has been depicted. More particularly, the classical methodologies for seismology have many vulnerabilities that require advanced support from other technologies. Accordingly, the hardware and software components of these technologies have been illustrated comprehensively. Third, the role of DCN and DCN-based modern systems for seismology have been discussed showing the meaning of each DCN element. Fourth, the transmission reliability, UDP protocol, TCP protocol, routing protocols, delays, media access techniques, and transmission of real-time monitoring data have been addressed. Fifth, the desirability of data communication-based advanced networks for seismology has been overviewed, such as using IoT and social media. Sixth, the optimization and seismology correlation has been exhibited. More specifically, two categories of optimization have been discussed: its role for seismic signals, and its role in prolonging the seismic networks. Seventh, an extensive overview of the AI utilization for seismology has been presented.

Due to being such a vulnerable system that still needs more enhancements and research cooperation, in the future direction, we do recommend employing modern technologies such as ML for EQs' detection, exploiting the fast booming of the IoT to overcome the classical monitoring system vulnerabilities, enhancing the role of EEWS, and finally implementing an integrating system relying on ML, IoT, and optimization techniques for effective disaster management and risk mitigation. In other words, such a system can be implemented over three phases starting with a basic alarm supported by the EEW. The second phase can be involved in disaster management. The third phase is risk mitigation.

References

[1] M. Elhadidy, M. S. Abdalzaher, and H. Gaber, "Up-to-date PSHA along the gulf of Aqaba-dead sea transform fault," *Soil Dyn. Earthq. Eng.*, vol. 148, 2021, Art. no. 106835.

[2] M. S. Abdalzaher, M. El-Hadidy, H. Gaber, and A. Badawy, "Seismic hazard maps of Egypt based on spatially smoothed seismicity model and recent seismotectonic models," *J. Afr. Earth Sci.*, vol. 170, 2020, Art. no. 103894.

[3] M. S. Abdalzaher, M. S. Soliman, S. M. El-Hady, A. Benslimane, and M. Elwekeil, "A deep learning model for earthquake parameters observation in IoT system-based earthquake early warning," *IEEE Internet Things J.*, vol. 9, no. 11, pp. 8412–8424, Jun. 2022.

[4] M. S. Abdalzaher and H. A. Elsayed, "Employing data communication networks for managing safer evacuation during earthquake disaster," *Simul. Model. Pract. Theory*, vol. 94, pp. 379–394, 2019.

[5] T.-D. Cao et al., "IoT services for solving critical problems in Vietnam: A research landscape and directions," *IEEE Internet Comput.*, vol. 20, no. 5, pp. 76–81, Sep./Oct. 2016.

[6] F. Alamdar, M. Kalantari, and A. Rajabifard, "Understanding the provision of multi-agency sensor information in disaster management: A case study on the australian state of victoria," *Int. J. Disaster Risk Reduction*, vol. 22, pp. 475–493, 2017.

[7] B.-R. Wu et al., "An integrated earthquake early warning system and its performance at schools in Taiwan," *J. Seismol.*, vol. 21, no. 1, pp. 165–180, 2017.

[8] Z. Wang and B. Zhao, "Automatic event detection and picking of p, s seismic phases for earthquake early warning and application for the 2008 wenchuan earthquake," *Soil Dyn. Earthq. Eng.*, vol. 97, pp. 172–181, 2017.

[9] S. Horiuchi et al., "Home seismometer for earthquake early warning," *Geophysical Res. Lett.*, vol. 36, no. 5, pp. 1–5, 2009.

[10] O. Hamdy, H. Gaber, M. S. Abdalzaher, and M. Elhadidy, "Identifying exposure of urban area to certain seismic hazard using machine learning and GIS: A case study of greater Cairo," *Sustainability*, vol. 14, no. 17, 2022, Art. no. 10722.

[11] M. S. Abdalzaher, S. S. Moustafa, H. Abdelhafiez, and W. Farid, "An optimized learning model augment analyst decisions for seismic source discrimination," *IEEE Trans. Geosci. Remote Sens.*, vol. 60, pp. 1–12, Sep. 2022, Art. no. 5920212.

[12] P. M. Shearer, *Introduction to Seismology*, 2nd ed. New York, NY, USA: Cambridge Univ. Press, 2009.

[13] S. Stein and M. Wysession, *An Introduction to Seismology, Earthquakes, and Earth Structure*. New York, NY, USA: Wiley, 2009.

[14] R. V. Allen, "Automatic earthquake recognition and timing from single traces," *Bull. Seismological Soc. Amer.*, vol. 68, no. 5, pp. 1521–1532, 1978.

[15] M. Leonard and B. Kennett, "Multi-component autoregressive techniques for the analysis of seismograms," *Phys. Earth Planet. Interiors*, vol. 113, no. 1–4, pp. 247–263, 1999.

[16] M. A. Shafiq, H. Di, and G. AlRegib, "A novel approach for automated detection of listric faults within migrated seismic volumes," *J. Appl. Geophys.*, vol. 155, pp. 94–101, 2018.

[17] G. AlRegib et al., "Subsurface structure analysis using computational interpretation and learning: A visual signal processing perspective," *IEEE Signal Process. Mag.*, vol. 35, no. 2, pp. 82–98, Mar. 2018.

[18] M. A. Shafiq, T. Alshawi, Z. Long, and G. AlRegib, "Salsi: A new seismic attribute for salt dome detection," in *Proc. IEEE Int. Conf. Acoust., Speech Signal Process.*, 2016, pp. 1876–1880.

[19] A. Masih, "An enhanced seismic activity observed due to climate change: Preliminary results from Alaska," in *Proc. IOP Conf. Ser.: Earth Environ. Sci.*, vol. 167, no. 1, 2018, Art. no. 012018.

[20] C.-H. Wang and N. Chen, "Are people equally exposed to seismic and climate-change-induced hazards? Evidence from the San Francisco Bay area," *Environ. Plan. B, Urban Anal. City Sci.*, 2022, Art. no. 23998083221100552.

[21] F. Jing and R. P. Singh, "Changes in tropospheric ozone associated with strong earthquakes and possible mechanism," *IEEE J. Sel. Topics Appl. Earth Observ. Remote Sens.*, vol. 14, pp. 5300–5310, May 2021.

[22] Z. Lv, T. Liu, X. Kong, C. Shi, and J. A. Benediktsson, "Landslide inventory mapping with bitemporal aerial remote sensing images based on the dual-path fully convolutional network," *IEEE J. Sel. Topics Appl. Earth Observ. Remote Sens.*, vol. 13, pp. 4575–4584, Mar. 2020.

[23] Z. Liu, J. Zhang, X. Li, and X. Chen, "Long-term resilience curve analysis of Wenchuan earthquake-affected counties using DMSP-OLS nighttime light images," *IEEE J. Sel. Topics Appl. Earth Observ. Remote Sens.*, vol. 14, pp. 10854–10874, Oct. 2021.

[24] F. Jing, R. P. Singh, Y. Cui, and K. Sun, "Microwave brightness temperature characteristics of three strong earthquakes in Sichuan province, China," *IEEE J. Sel. Topics Appl. Earth Observ. Remote Sens.*, vol. 13, pp. 513–522, Jan. 2020.

[25] T. Chen, X. Zheng, R. Niu, and A. Plaza, "Open-pit mine area mapping with Gaofen-2 satellite images using u-net+," *IEEE J. Sel. Topics Appl. Earth Observ. Remote Sens.*, vol. 15, pp. 3589–3599, Apr. 2022.

[26] B. Zhang et al., "Progress and challenges in intelligent remote sensing satellite systems," *IEEE J. Sel. Topics Appl. Earth Observ. Remote Sens.*, vol. 15, pp. 1814–1822, Feb. 2022.

[27] Y. Qi, L. Wu, M. He, and W. Mao, "Spatio-temporally weighted two-step method for retrieving seismic MBT anomaly: May 2008 Wenchuan earthquake sequence being a case," *IEEE J. Sel. Topics Appl. Earth Observ. Remote Sens.*, vol. 13, pp. 382–391, Jan. 2020.

[28] B. Su et al., "The outgoing longwave radiation analysis of medium and strong earthquakes," *IEEE J. Sel. Topics Appl. Earth Observ. Remote Sens.*, vol. 14, pp. 6962–6973, Jun. 2021.

[29] L. L. Peterson and B. S. Davie, *Computer Networks: A Systems Approach*. New York, NY, USA: Elsevier, 2007.

[30] B. A. Forouzan, *TCP/IP Protocol Suite*. New York, NY, USA: McGraw-Hill Higher Education, 2002.

[31] S. Dou et al., "Distributed acoustic sensing for seismic monitoring of the near surface: A traffic-noise interferometry case study," *Sci. Rep.*, vol. 7, no. 1, pp. 1–12, 2017.

[32] M. Avvenuti, S. Cresci, A. Marchetti, C. Meletti, and M. Tesconi, "Predictability or early warning: Using social media in modern emergency response," *IEEE Internet Comput.*, vol. 20, no. 6, pp. 4–6, Nov./Dec. 2016.

[33] D. Zekkos, A. Tsavalas-Hardy, G. M. Mandilaras, and K. A. Tsantilas, "Using social media to assess earthquake impact on people and infrastructure: Examples from earthquakes in 2018," in *Proc. 2nd Int. Conf. Natural Hazards Infrastructure*, 2019, pp. 1–10.

[34] D. Murthy and A. J. Gross, "Social media processes in disasters: Implications of emergent technology use," *Social Sci. Res.*, vol. 63, pp. 356–370, 2017.

[35] J. Sutton, E. S. Spiro, B. Johnson, S. Fitzhugh, B. Gibson, and C. T. Butts, "Warning tweets: Serial transmission of messages during the warning phase of a disaster event," *Inf., Commun. Soc.*, vol. 17, no. 6, pp. 765–787, 2014.

[36] J. Yin, A. Lampert, M. Cameron, B. Robinson, and R. Power, "Using social media to enhance emergency situation awareness," *IEEE Intell. Syst.*, vol. 27, no. 6, pp. 52–59, Nov./Dec. 2012.

[37] S. E. Middleton, L. Middleton, and S. Modafferi, "Real-time crisis mapping of natural disasters using social media," *IEEE Intell. Syst.*, vol. 29, no. 2, pp. 9–17, Mar./Apr. 2014.

[38] D. C. Bowden, P. S. Earle, M. Guy, and G. Smoczyk, "Twitter seismology: Earthquake monitoring and response in a social world," in *Proc. AGU Fall Meeting Abstr.*, 2011, pp. 708–715.

[39] G. Mei, N. Xu, J. Qin, B. Wang, and P. Qi, "A survey of Internet of Things (IoT) for geohazard prevention: Applications, technologies, and challenges," *IEEE Internet Things J.*, vol. 7, no. 5, pp. 4371–4386, May 2020.

[40] X. Li, R. Lu, X. Liang, X. Shen, J. Chen, and X. Lin, "Smart community: An Internet of Things application," *IEEE Commun. Mag.*, vol. 49, no. 11, pp. 68–75, Nov. 2011.

[41] E. Ghamry et al., "Integrating pre-earthquake signatures from different precursor tools," *IEEE Access*, vol. 9, pp. 33268–33283, 2021.

[42] S. S. Moustafa, M. S. Abdalzaher, M. Naeem, and M. M. Fouda, "Seismic hazard and site suitability evaluation based on multicriteria decision analysis," *IEEE Access*, vol. 10, pp. 69511–69530, 2022.

[43] M. De Sanctis, E. Cianca, G. Araniti, I. Bisio, and R. Prasad, "Satellite communications supporting internet of remote things," *IEEE Internet Things J.*, vol. 3, no. 1, pp. 113–123, Feb. 2016.

[44] C. Mouradian, N. T. Jahromi, and R. H. Glitho, "NFV and SDN-based distributed IoT gateway for large-scale disaster management," *IEEE Internet Things J.*, vol. 5, no. 5, pp. 4119–4131, Oct. 2018.

[45] N.-H. Bao, M. Kuang, S. Sahoo, G.-P. Li, and Z.-Z. Zhang, "Early-warning-time-based virtual network live evacuation against disaster threats," *IEEE Internet Things J.*, vol. 7, no. 4, pp. 2869–2876, Apr. 2020.

[46] J. N. Brune, "Implications of earthquake triggering and rupture propagation for earthquake prediction based on premonitory phenomena," *J. Geophysical Res., Solid Earth*, vol. 84, no. B5, pp. 2195–2198, 1979.

[47] Y. Fukao and M. Furumoto, "Hierarchy in earthquake size distribution," *Phys. Earth Planet. Interiors*, vol. 37, no. 2, pp. 149–168, 1985.

[48] Z. Li, Z. Peng, D. Hollis, L. Zhu, and J. McClellan, "High-resolution seismic event detection using local similarity for large-n arrays," *Sci. Rep.*, vol. 8, no. 1, pp. 1–10, 2018.

[49] E. L. Olson and R. M. Allen, "The deterministic nature of earthquake rupture," *Nature*, vol. 438, no. 7065, pp. 212–215, 2005.

[50] S. Poslad, S. E. Middleton, F. Chaves, R. Tao, O. Necmioglu, and U. Bügel, "A semantic IoT early warning system for natural environment crisis management," *IEEE Trans. Emerg. Topics Comput.*, vol. 3, no. 2, pp. 246–257, Jun. 2015.

[51] K. Chung and R. C. Park, "P2p cloud network services for IoT based disaster situations information," *Peer-to-Peer Netw. Appl.*, vol. 9, no. 3, pp. 566–577, 2016.

[52] M. M. Salim, H. A. ElSayed, M. S. Abdalzaher, and M. M. Fouda, "RF energy harvesting dependency for power optimized two-way relaying D2D communication," in *Proc. IEEE Int. Conf. Internet Things Intell. Syst.*, 2022, pp. 1–7.

[53] A. Zambrano, I. Perez, C. Palau, and M. Esteve, "Technologies of Internet of Things applied to an earthquake early warning system," *Future Gener. Comput. Syst.*, vol. 75, pp. 206–215, 2017.

[54] S. M. Mousavi and G. C. Beroza, "Bayesian-deep-learning estimation of earthquake location from single-station observations," *IEEE Trans. Geosci. Remote Sens.*, vol. 58, no. 11, pp. 8211–8224, Nov. 2020.

[55] M. S. Abdalzaher, M. M. Fouda, and M. I. Ibrahem, "Data privacy preservation and security in smart metering systems: A survey," *Energies*, vol. 15, no. 19, 2022, Art. no. 7419.

[56] M. S. Abdalzaher, M. M. Salim, H. A. ElSayed, and M. M. Fouda, "Machine learning benchmarking for secured IoT smart systems," *Proc. IEEE Int. Conf. Internet Things Intell. Syst.*, 2022, pp. 1–7.

[57] M. Elwekeil, M. S. Abdalzaher, and K. Seddik, "Prolonging smart grid network lifetime through optimising number of sensor nodes and packet length," *IET Commun.*, vol. 13, no. 16, pp. 2478–2484, 2019.

[58] F. Delbos, J. C. Gilbert, R. Glowinski, and D. Sinoquet, "Constrained optimization in seismic reflection tomography: A Gauss-Newton augmented Lagrangian approach," *Geophysical J. Int.*, vol. 164, no. 3, pp. 670–684, 2006.

[59] M. Bosch, "The optimization approach to lithological tomography: Combining seismic data and petrophysics for porosity prediction," *Geophysics*, vol. 69, no. 5, pp. 1272–1282, 2004.

[60] W. Hu, A. Abubakar, and T. M. Habashy, "Joint electromagnetic and seismic inversion using structural constraints," *Geophysics*, vol. 74, no. 6, pp. R99–R109, 2009.

[61] I. Epanomeritakis, V. Akçelik, O. Ghattas, and J. Bielak, "A newton-CG method for large-scale three-dimensional elastic full-waveform seismic inversion," *Inverse Problems*, vol. 24, no. 3, 2008, Art. no. 034015.

[62] S. Gholizadeh, M. Danesh, and C. Gheyratmand, "A new newton metaheuristic algorithm for discrete performance-based design optimization of steel moment frames," *Comput. Struct.*, vol. 234, 2020, Art. no. 106250.

[63] R. Brossier, S. Operto, and J. Virieux, "Seismic imaging of complex onshore structures by 2D elastic frequency-domain full-waveform inversion," *Geophysics*, vol. 74, no. 6, pp. WCC105–WCC118, 2009.

[64] T. van Leeuwen and F. J. Herrmann, "3d frequency-domain seismic inversion with controlled sloppiness," *SIAM J. Sci. Comput.*, vol. 36, no. 5, pp. S192–S217, 2014.

[65] M. Dadashpour, D. Echeverría-Ciaurri, J. Kleppe, and M. Landrø, "Porosity and permeability estimation by integration of production and time-lapse near and far offset seismic data," *J. Geophys. Eng.*, vol. 6, no. 4, pp. 325–344, 2009.

[66] C. Boehm and M. Ulbrich, "A semismooth newton-cg method for constrained parameter identification in seismic tomography," *SIAM J. Sci. Comput.*, vol. 37, no. 5, pp. S334–S364, 2015.

[67] T.-Y. Lee, K.-J. Chung, and H. Chang, "A new procedure for nonlinear dynamic analysis of structures under seismic loading based on equivalent nodal secant stiffness," *Int. J. Struct. Stability Dyn.*, vol. 18, no. 3, 2018, Art. no. 1850043.

[68] E. Heredia-Zavoni, A. Zeballos, and L. Esteva, "Theoretical models and recorded response in the estimation of cumulative seismic damage on non-linear structures," *Earthq. Eng. Struct. Dyn.*, vol. 29, no. 12, pp. 1779–1796, 2000.

[69] M. Capistran, M. A. Moreles, and J. Pena, "On full seismic waveform inversion by descent methods in a lattice," *Appl. Math*, vol. 6, no. 2, pp. 193–203, 2012.

[70] R. S. Olivito and S. Porzio, "A new multi-control-point pushover methodology for the seismic assessment of historic masonry buildings," *J. Building Eng.*, vol. 26, 2019, Art. no. 100926.

[71] Y. Wang and T. D. O'Rourke, "Interpretation of secant shear modulus degradation characteristics from pressuremeter tests," *J. Geotechnical Geoenvironmental Eng.*, vol. 133, no. 12, pp. 1556–1566, 2007.

[72] J. Tromp, D. Komatitsch, and Q. Liu, "Spectral-element and adjoint methods in seismology," *Commun. Comput. Phys.*, vol. 3, no. 1, pp. 1–32, 2008.

[73] M. Papadrakakis, H. Mouzakis, N. Plevris, and S. Bitzarakis, "A lagrange multiplier solution method for pounding of buildings during earthquakes," *Earthq. Eng. Struct. Dyn.*, vol. 20, no. 11, pp. 981–998, 1991.

[74] Q. Liu and J. Tromp, "Finite-frequency kernels based on adjoint methods," *Bull. Seismological Soc. Amer.*, vol. 96, no. 6, pp. 2383–2397, 2006.

[75] N. Kreimer and M. D. Sacchi, "Nuclear norm minimization and tensor completion in exploration seismology," in *Proc. IEEE Int. Conf. Acoust., Speech Signal Process.*, 2013, pp. 4275–4279.

[76] S. Treitel and L. Lines, "Linear inverse theory and deconvolution," *Geophysics*, vol. 47, no. 8, pp. 1153–1159, 1982.

[77] F. J. Herrmann, M. P. Friedlander, and O. Yilmaz, "Fighting the curse of dimensionality: Compressive sensing in exploration seismology," *IEEE Signal Process. Mag.*, vol. 29, no. 3, pp. 88–100, May 2012.

[78] Y. Cai, T. He, and R. Wang, "Numerical simulation of dynamic process of the Tangshan earthquake by a new method–LDDA," *Pure Appl. Geophys.*, vol. 157, no. 11, pp. 2083–2104, 2000.

[79] B. R. Julian and G. Foulger, "Earthquake mechanisms from linear-programming inversion of seismic-wave amplitude ratios," *Bull. Seismological Soc. America*, vol. 86, no. 4, pp. 972–980, 1996.

[80] E. Ladopoulos, "Hydrocarbon reserves exploration by real-time expert seismology and non-linear singular integral equations," *Int. J. Oil, Gas Coal Technol.*, vol. 5, no. 4, pp. 299–315, 2012.

[81] E. Ladopoulos, "Non-linear singular integral equations & real-time expert seismology for petroleum reserves exploration," *Univ. J. Eng. Mech.*, vol. 32, pp. 16–32, 2014.

[82] S. Levv, D. Oldenburg, and J. Wang, "Subsurface imaging using magnetotelluric data," *Geophysics*, vol. 53, no. 1, pp. 104–117, 1988.

[83] G. Nolet, *Seismic Tomography: With Applications in Global Seismology and Exploration Geophysics*, vol. 5. New York, NY, USA: Springer, 1987.

[84] J. A. Connolly, "Computation of phase equilibria by linear programming: A tool for geodynamic modeling and its application to subduction zone decarbonation," *Earth Planet. Sci. Lett.*, vol. 236, no. 1/2, pp. 524–541, 2005.

[85] P. Palo, S. S. Panda, R. Mandai, and A. Routray, "Sparse layer inversion using linear programming approach," in *Proc. IEEE Int. Geosci. Remote Sens. Symp.*, 2019, pp. 1923–1926.

[86] E. L. Geist and T. Parsons, "Distribution of earthquakes on a branching fault system using integer programming and greedy-sequential methods," *Geochemistry, Geophys., Geosystems*, vol. 21, no. 9, 2020, Art. no. e2020GC008964.

[87] E. L. Geist and T. Parsons, "Determining on-fault magnitude distributions for a connected, multi-fault system," in *Proc. AGU Fall Meeting Abstr.*, 2017, vol. 2017, pp. S11B–0579.

[88] E. L. Geist and U. S. Ten Brink, "Earthquake distributions along northern caribbean faults are sensitive to assumptions of plate boundary coupling and segmentation," in *Proc. AGU Fall Meeting Abstr.*, 2020, vol. 2020, pp. T054–0013.

[89] Y. Ohsawa and M. Yachida, "Discover risky active faults by indexing an earthquake sequence," in *Proc. Int. Conf. Discov. Sci.*, 1999, pp. 208–219.

[90] E. L. Geist and T. Parsons, "A combinatorial approach to determine earthquake magnitude distributions on a variable slip-rate fault," *Geophysical J. Int.*, vol. 219, no. 2, pp. 734–752, 2019.

[91] J. A. Paul and L. MacDonald, "Location and capacity allocations decisions to mitigate the impacts of unexpected disasters," *Eur. J. Oper. Res.*, vol. 251, no. 1, pp. 252–263, 2016.

[92] Y. Huang and W. Pang, "Optimization of resilient biofuel infrastructure systems under natural hazards," *J. Energy Eng.*, vol. 140, no. 2, 2014, Art. no. 04013017.

[93] A. J. Siade, M. Putti, and W. W.-G. Yeh, "Reduced order parameter estimation using quasilinearization and quadratic programming," *Water Resour. Res.*, vol. 48, no. 6, pp. 1–14, 2012.

[94] M. Soltanolkotabi, *Algorithms and Theory for Clustering and Nonconvex Quadratic Program.* Stanford, CA, USA: Stanford Univ., 2014.

[95] T. Eken, Z. H. Shomali, R. Roberts, and R. Bödvarsson, "Upper-mantle structure of the baltic shield below the Swedish national seismological network (SNSN) resolved by teleseismic tomography," *Geophysical J. Int.*, vol. 169, no. 2, pp. 617–630, 2007.

[96] K. Shimazaki, "Pre-seismic crustal deformation caused by an underthrusting oceanic plate, in Eastern Hokkaido, Japan," *Phys. Earth Planet. Interiors*, vol. 8, no. 2, pp. 148–157, 1974.

[97] F. Yerlikaya-Özkurt, A. Askan, and G.-W. Weber, "An alternative approach to the ground motion prediction problem by a non-parametric adaptive regression method," *Eng. Optim.*, vol. 46, no. 12, pp. 1651–1668, 2014.

[98] Z. H. Shomali, F. Keshvari, J. Hassanzadeh, and N. Mirzaei, "Lithospheric structure beneath the Zagros collision zone resolved by nonlinear teleseismic tomography," *Geophysical J. Int.*, vol. 187, no. 1, pp. 394–406, 2011.

[99] H. Motamed, M. Ghafory-Ashtiany, and K. Amini-Hosseini, "An earthquake risk-sensitive model for spatial land-use allocation," in *Proc. 15th World Conf. Earthq. Eng.*, Lisbon, Portugal, 2012, pp. 1–8.

[100] M. A. C. Tura, L. R. Johnson, E. L. Majer, and J. E. Peterson, "Application of diffraction tomography to fracture detection," *Geophysics*, vol. 57, no. 2, pp. 245–257, 1992.

[101] F. Yerlikaya-Özkurt, A. Askan, and G.-W. Weber, "A hybrid computational method based on convex optimization for outlier problems: Application to earthquake ground motion prediction," *Informatica*, vol. 27, no. 4, pp. 893–910, 2016.

[102] S. Zhou and X. Chen, "Inversion of near-field waveform data for earthquake source rupture process (i): Method and numerical test," *Sci. China Ser. D: Earth Sci.*, vol. 46, no. 11, pp. 1089–1102, 2003.

[103] D. Vasco, "Moment-tensor invariants: Searching for non-double-couple earthquakes," *Bull. Seismological Soc. Amer.*, vol. 80, no. 2, pp. 354–371, 1990.

[104] Y. Li, J. Xiao, and Y. Zhu, "Estimation of magnetic particle size distribution for ferrofluids based on nonlinear programming optimization and an improved Bayesian method," *J. Magnetism Magn. Mater.*, vol. 482, pp. 99–107, 2019.

[105] A. Tarantola, *Inverse Problem Theory and Methods for Model Parameter Estimation*. Philadelphia, PA, USA: SIAM, 2005.

[106] D. C. Bowman and J. M. Lees, "The Hilbert-Huang transform: A high resolution spectral method for nonlinear and nonstationary time series," *Seismological Res. Lett.*, vol. 84, no. 6, pp. 1074–1080, 2013.

[107] E. Ladopoulos, "General form of non-linear real-time expert seismology for oil and gas reserves exploration," *Univ. J. Petrol. Sci.*, vol. 1, no. 1, pp. 1–14, 2013.

[108] G. Barbarosoğlu and Y. Arda, "A two-stage stochastic programming framework for transportation planning in disaster response," *J. Oper. Res. Soc.*, vol. 55, no. 1, pp. 43–53, 2004.

[109] C. Liu, Y. Fan, and F. Ordóñez, "A two-stage stochastic programming model for transportation network protection," *Comput. Oper. Res.*, vol. 36, no. 5, pp. 1582–1590, 2009.

[110] S. Rath, M. Gendreau, and W. J. Gutjahr, "Bi-objective stochastic programming models for determining depot locations in disaster relief operations," *Int. Trans. Oper. Res.*, vol. 23, no. 6, pp. 997–1023, 2016.

[111] M. R. Zolfaghari and E. Peyghaleh, "Implementation of equity in resource allocation for regional earthquake risk mitigation using two-stage stochastic programming," *Risk Anal.*, vol. 35, no. 3, pp. 434–458, 2015.

[112] Y. Fan, C. Liu, R. Lee, and A. S. Kiremidjian, "Highway network retrofit under seismic hazard," *J. Infrastructure Syst.*, vol. 16, no. 3, pp. 181–187, 2010.

[113] W. Schneider Jr, K. A. Ranzinger, A. Balch, and C. Kruse, "A dynamic programming approach to first arrival traveltime computation in media with arbitrarily distributed velocities," *Geophysics*, vol. 57, no. 1, pp. 39–50, 1992.

[114] Y.-D. Huang and M. BArkat, "A dynamic programming algorithm for the maximum likelihood localization of multiple sources," *IEEE Trans. Antennas Propag.*, vol. 40, no. 9, pp. 1023–1030, Sep. 1992.

[115] K. R. Anderson and J. E. Gaby, "Dynamic waveform matching," *Inf. Sci.*, vol. 31, no. 3, pp. 221–242, 1983.

[116] E. Darby and N. S. Neidell, "Application of dynamic programming to the problem of plane wave propagation in a layered medium," *Geophysics*, vol. 31, no. 6, pp. 1037–1048, 1966.

[117] C. Tang et al., "Discovering tendency association between objects with relaxed periodicity and its application in seismology," in *Proc. Int. Comput. Sci. Conf.*, 1999, pp. 51–62.

[118] S. K. Nath, S. Chakraborty, S. K. Singh, and N. Ganguly, "Velocity inversion in cross-hole seismic tomography by counter-propagation neural network, genetic algorithm and evolutionary programming techniques," *Geophysical J. Int.*, vol. 138, no. 1, pp. 108–124, 1999.

[119] Y. Takenaka, N. Funabiki, and S. Nishikawa, "A proposal of" neuron mask" in neural network algorithm for combinatorial optimization problems," in *Proc. Int. Conf. Neural Netw.*, 1997, vol. 2, pp. 1289–1294.

[120] E. L. Geist and U. S. ten Brink, "Earthquake magnitude distributions on northern caribbean faults from combinatorial optimization models," *J. Geophysical Res., Solid Earth*, vol. 126, no. 10, 2021, Art. no. e2021JB022050.

[121] E.-V. Pikoulis and E. Z. Psarakis, "A new blind beamforming technique for the alignment and enhancement of seismic signals," in *Proc. 26th Eur. Signal Process. Conf.*, 2018, pp. 2385–2389.

[122] L. Schmidt, C. Hegde, P. Indyk, L. Lu, X. Chi, and D. Hohl, "Seismic feature extraction using steiner tree methods," in *Proc. IEEE Int. Conf. Acoust., Speech Signal Process.*, 2015, pp. 1647–1651.

[123] G. Si-Yuan, D. Lin-Ming, M. Xiao-Ping, H. Jiang, and L. Yan-Gao, "Study on the improvement of the microseismic network configuration for San He-Jian coal mine," *Procedia Eng.*, vol. 26, pp. 1398–1405, 2011.

[124] Y.-M. Wu, L. Zhao, C.-H. Chang, and Y.-J. Hsu, "Focal-mechanism determination in Taiwan by genetic algorithm," *Bull. Seismological Soc. Amer.*, vol. 98, no. 2, pp. 651–661, 2008.

[125] J. F. Lawrence and D. A. Wiens, "Combined receiver-function and surface wave phase-velocity inversion using a Niching genetic algorithm: Application to Patagonia," *Bull. Seismological Soc. Amer.*, vol. 94, no. 3, pp. 977–987, 2004.

[126] S.-J. Chang, C.-E. Baag, and C. A. Langston, "Joint analysis of teleseismic receiver functions and surface wave dispersion using the genetic algorithm," *Bull. Seismological Soc. Amer.*, vol. 94, no. 2, pp. 691–704, 2004.

[127] S. Pezeshk and M. Zarrabi, "A new inversion procedure for spectral analysis of surface waves using a genetic algorithm," *Bull. Seismological Soc. Amer.*, vol. 95, no. 5, pp. 1801–1808, 2005.

[128] G. Suresh, S. Jain, and S. Bhattacharya, "Lithosphere of indus block in the northwest Indian subcontinent through genetic algorithm inversion of surface-wave dispersion," *Bull. Seismological Soc. Amer.*, vol. 98, no. 4, pp. 1750–1755, 2008.

[129] W. Jiang, X. Tao, and Z. Tao, "Seismology-based hybrid ground motion prediction models of PGA in Sichuan, China," *Soil Dyn. Earthq. Eng.*, vol. 156, 2022, Art. no. 107220.

[130] P. Omidian and N. Khaji, "A multi-objective optimization framework for seismic resilience enhancement of typical existing RC buildings," *J. Building Eng.*, vol. 52, 2022, Art. no. 104361.

[131] E. Büyük, "Pareto-based multiobjective particle swarm optimization: Examples in geophysical modeling," in *Optimisation Algorithms and Swarm Intelligence*, London, U.K.: IntechOpen, 2021.

[132] A. Nicknam, A. Hosseini, H. H. Jamnani, and M. Barkhordari, "Reproducing fling-step and forward directivity at near source site using of multi-objective particle swarm optimization and multi taper," *Earthq. Eng. Eng. Vib.*, vol. 12, no. 4, pp. 529–540, 2013.

[133] X. Y. Zhang, X. Li, and X. Lin, "The data mining technology of particle swarm optimization algorithm in earthquake prediction," in *Advanced Materials Research*, vol. 989. Baech, Switzerland: Trans. Tech. Publ., 2014, pp. 1570–1573.

[134] S. SoltaniMoghadam, M. Tatar, and A. Komeazi, "An improved 1-d crustal velocity model for the central Alborz (Iran) using particle swarm optimization algorithm," *Phys. Earth Planet. Interiors*, vol. 292, pp. 87–99, 2019.

[135] K. Deep, A. Yadav, and S. Kumar, "Improving local and regional earthquake locations using an advance inversion technique: Particle swarm optimization," *World J. Model. Simul.*, vol. 8, no. 2, pp. 135–141, 2012.

[136] A. Askan, V. Akcelik, J. Bielak, and O. Ghattas, "Full waveform inversion for seismic velocity and anelastic losses in heterogeneous structures," *Bull. Seismological Soc. Amer.*, vol. 97, no. 6, pp. 1990–2008, 2007.

[137] S. Zverev and M. Polyanskii, "Structural variations along the Kuril-Kamchatka trench and a possible relation to seismicity," *J. Volcanol. Seismol.*, vol. 2, no. 1, pp. 1–15, 2008.

[138] P. Lemenkova, "Gmt-based geological mapping and assessment of the bathymetric variations of the Kuril-Kamchatka trench, Pacific Ocean," *Natural Eng. Sci.*, vol. 5, no. 1, pp. 1–17, 2020.

[139] S. K. Pullammanappallil and J. N. Louie, "A generalized simulated-annealing optimization for inversion of first-arrival times," *Bull. Seismological Soc. Amer.*, vol. 84, no. 5, pp. 1397–1409, 1994.

[140] K. Mosegaard and P. D. Vestergaard, "A simulated annealing approach to seismic model optimization with sparse prior information1," *Geophysical Prospecting*, vol. 39, no. 5, pp. 599–611, 1991.

[141] M. Martınez, X. Lana, J. Olarte, J. Badal, and J. Canas, "Inversion of rayleigh wave phase and group velocities by simulated annealing," *Phys. Earth Planet. Interiors*, vol. 122, no. 1/2, pp. 3–17, 2000.

[142] K. S. Beaty, D. R. Schmitt, and M. Sacchi, "Simulated annealing inversion of multimode Rayleigh wave dispersion curves for geological structure," *Geophysical J. Int.*, vol. 151, no. 2, pp. 622–631, 2002.

[143] C. R. Conti, M. Roisenberg, G. S. Neto, and M. J. Porsani, "Fast seismic inversion methods using ant colony optimization algorithm," *IEEE Geosci. Remote Sens. Lett.*, vol. 10, no. 5, pp. 1119–1123, Sep. 2013.

[144] X. Shao, X. Li, L. Li, and X. Hu, "The application of ant-colony clustering algorithm to earthquake prediction," in *Advances in Electronic Engineering, Communication and Management*, vol. 2. Berlin, Germany: Springer, 2012, pp. 145–150.

[145] O. Mishra, P. Dutta, and M. Naskar, "Relationship between earthquake fault triggering and societal behavior using ant colony optimization," *Adv. Phys. Theories Appl.*, vol. 26, pp. 99–108, 2013.

[146] G.-q. Shi, X.-f. He, and R.-y. Xiao, "Acquiring three-dimensional deformation of Kilauea's south flank from GPS and dinsar integration based on the ant colony optimization," *IEEE Geosci. Remote Sens. Lett.*, vol. 12, no. 12, pp. 2506–2510, Dec. 2015.

[147] E. Forcael, V. González, F. Orozco, S. Vargas, A. Pantoja, and P. Moscoso, "Ant colony optimization model for tsunamis evacuation routes," *Comput.-Aided Civil Infrastructure Eng.*, vol. 29, no. 10, pp. 723–737, 2014.

[148] L. Huang, X. Li, and D. Liu, "Microseismic location method using ω penalty function based ant colony optimization," in *Proc. 12th Int. Comput. Eng. Conf.*, 2016, pp. 208–212.

[149] H. Duwiquet, L. Guillou-Frottier, L. Arbaret, M. Bellanger, T. Guillon, and M. J. Heap, "Crustal fault zones (CFZ) as geothermal power systems: A preliminary 3D THM model constrained by a multidisciplinary approach," *Geofluids*, vol. 2021, pp. 1–24, 2021.

[150] W. W. Symes, "A differential semblance algorithm for the inverse problem of reflection seismology," *Comput. Math. Appl.*, vol. 22, no. 4, pp. 147–178, 1991.

[151] M. M. Hason, A. N. Hanoon, and A. A. Abdulhameed, "Particle swarm optimization technique based prediction of peak ground acceleration of Iraq's tectonic regions," *J. King Saud Univ. - Eng. Sci.*, to be published, doi: 10.1016/j.jksues.2021.06.004.

[152] M. Muratov, V. Ryazanov, V. Biryukov, D. Petrov, and I. Petrov, "Inverse problems of heterogeneous geological layers exploration seismology solution by methods of machine learning," *Lobachevskii J. Math.*, vol. 42, no. 7, pp. 1728–1737, 2021.

[153] M. S. Abdalzaher, O. Muta, K. Seddik, A. Abdel-Rahman, and H. Furukawa, "B-18-40 a simplified Stackelberg game approach for securing data trustworthiness in wireless sensor networks," in *Proc. IEICE Gen. Conf.*, 2016, p. 538.
[154] M. S. Abdalzaher and O. Muta, "Employing game theory and TDMA protocol to enhance security and manage power consumption in wsns-based cognitive radio," *IEEE Access*, vol. 7, pp. 132923–132936, 2019.
[155] M. S. Abdalzaher, K. Seddik, and O. Muta, "An effective Stackelberg game for high-assurance of data trustworthiness in WSNs," in *Proc. IEEE Symp. Comput. Commun.*, 2017, pp. 1257–1262.
[156] M. S. Abdalzaher and O. Muta, "A game-theoretic approach for enhancing security and data trustworthiness in IoT applications," *IEEE Internet Things J.*, vol. 7, no. 11, pp. 11250–11261, Nov. 2020.
[157] M. S. Abdalzaher, L. Samy, and O. Muta, "Non-zero-sum game-based trust model to enhance wireless sensor networks security for IoT applications," *IET Wireless Sensor Syst.*, vol. 9, no. 4, pp. 218–226, 2019.
[158] M. S. Abdalzaher, K. Seddik, M. Elsabrouty, O. Muta, H. Furukawa, and A. Abdel-Rahman, "Game theory meets wireless sensor networks security requirements and threats mitigation: A survey," *Sensors*, vol. 16, no. 7, 2016, Art. no. 1003.
[159] M. S. Abdalzaher, K. Seddik, and O. Muta, "Using stackelberg game to enhance cognitive radio sensor networks security," *IET Commun.*, vol. 11, no. 9, pp. 1503–1511, 2017.
[160] M. S. Abdalzaher, K. Seddik, O. Muta, and A. Abdelrahman, "Using stackelberg game to enhance node protection in WSNs," in *Proc. 13th IEEE Annu. Consum. Commun. Netw. Conf.*, 2016, pp. 853–856.
[161] M. S. Abdalzaher, K. Seddik, and O. Muta, "Using repeated game for maximizing high priority data trustworthiness in wireless sensor networks," in *Proc. IEEE Symp. Comput. Commun.*, 2017, pp. 552–557.
[162] "Tmote sky: Datasheet," [Online]. Available: https://insense.cs.st-andrews.ac.uk/files/2013/04/tmote-sky-datasheet.pdf
[163] V. C. Gungor, B. Lu, and G. P. Hancke, "Opportunities and challenges of wireless sensor networks in smart grid," *IEEE Trans. Ind. Electron.*, vol. 57, no. 10, pp. 3557–3564, Oct. 2010.
[164] W. Zhu, S. M. Mousavi, and G. C. Beroza, "Seismic signal denoising and decomposition using deep neural networks," *IEEE Trans. Geosci. Remote Sens.*, vol. 57, no. 11, pp. 9476–9488, Nov. 2019.
[165] L. Yang, X. Liu, W. Zhu, L. Zhao, and G. C. Beroza, "Toward improved urban earthquake monitoring through deep-learning-based noise suppression," *Sci. Adv.*, vol. 8, no. 15, 2022, Art. no. eabl3564.
[166] F. Wang, B. Yang, Y. Wang, and M. Wang, "Learning from noisy data: An unsupervised random denoising method for seismic data using model-based deep learning," *IEEE Trans. Geosci. Remote Sens.*, vol. 60, pp. 1–14, Apr. 2022, Art. no. 5913314.
[167] F. Qian, Z. Liu, Y. Wang, Y. Zhou, and G. Hu, "Ground truth-free 3-D seismic random noise attenuation via deep tensor convolutional neural networks in the time-frequency domain," *IEEE Trans. Geosci. Remote Sens.*, vol. 60, pp. 1–17, Feb. 2022, Art. no. 5911317.
[168] A. Novoselov, P. Balazs, and G. Bokelmann, "Sedenoss: Separating and denoising seismic signals with dual-path recurrent neural network architecture," *J. Geophysical Res.: Solid Earth*, vol. 127, no. 3, 2022, Art. no. e2021JB023183.
[169] S. S. Moustafa, M. S. Abdalzaher, F. Khan, M. Metwaly, E. A. Elawadi, and N. S. Al-Arifi, "A quantitative site-specific classification approach based on affinity propagation clustering," *IEEE Access*, vol. 9, pp. 155297–155313, 2021.
[170] S. M. Mousavi, W. Zhu, W. Ellsworth, and G. Beroza, "Unsupervised clustering of seismic signals using deep convolutional autoencoders," *IEEE Geosci. Remote Sens. Lett.*, vol. 16, no. 11, pp. 1693–1697, Nov. 2019.
[171] P. Anbazhagan, K. Srilakshmi, K. Bajaj, S. S. Moustafa, and N. S. Al-Arifi, "Determination of seismic site classification of seismic recording stations in the Himalayan region using HVSR method," *Soil Dyn. Earthq. Eng.*, vol. 116, pp. 304–316, 2019.
[172] R. Steinmann, L. Seydoux, E. Beaucé, and M. Campillo, "Hierarchical exploration of continuous seismograms with unsupervised learning," *J. Geophysical Res.: Solid Earth*, vol. 127, no. 1, 2022, Art. no. e2021JB022455.
[173] T. Perol, M. Gharbi, and M. Denolle, "Convolutional neural network for earthquake detection and location," *Sci. Adv.*, vol. 4, no. 2, 2018, Art. no. e1700578.
[174] Q. Zhang, W. Zhang, X. Wu, J. Zhang, W. Kuang, and X. Si, "Deep learning for efficient microseismic location using source migration-based imaging," *J. Geophysical Res., Solid Earth*, vol. 127, no. 3, 2022, Art. no. e2021JB022649.
[175] T. Bai and P. Tahmasebi, "Attention-based LSTM-FCN for earthquake detection and location," *Geophysical J. Int.*, vol. 228, no. 3, pp. 1568–1576, 2022.
[176] S. M. Mousavi and G. C. Beroza, "A machine-learning approach for earthquake magnitude estimation," *Geophysical Res. Lett.*, vol. 47, no. 1, 2020, Art. no. e2019GL085976.
[177] J. Zhu, S. Li, Q. Ma, B. He, and J. Song, "Support vector machine-based rapid magnitude estimation using transfer learning for the Sichuan–Yunnan region, China," *Bull. Seismological Soc. Amer.*, vol. 112, no. 2, pp. 894–904, 2022.
[178] R. M. Dokht, H. Kao, R. Visser, and B. Smith, "Seismic event and phase detection using time–frequency representation and convolutional neural networks," *Seismological Res. Lett.*, vol. 90, no. 2A, pp. 481–490, 2019.
[179] S. M. Mousavi, W. Zhu, Y. Sheng, and G. C. Beroza, "Cred: A deep residual network of convolutional and recurrent units for earthquake signal detection," *Sci. Rep.*, vol. 9, no. 1, pp. 1–14, 2019.
[180] M. Zhao, J. Ma, H. Chang, and S. Chen, "General seismic wave and phase detection software driven by deep learning," *Earthq. Res. Adv.*, vol. 1, no. 3, 2021, Art. no. 100029.
[181] Y. Wu, Y. Lin, Z. Zhou, D. C. Bolton, J. Liu, and P. Johnson, "Deepdetect: A cascaded region-based densely connected network for seismic event detection," *IEEE Trans. Geosci. Remote Sens.*, vol. 57, no. 1, pp. 62–75, Jan. 2019.
[182] Y. Chen, G. Zhang, M. Bai, S. Zu, Z. Guan, and M. Zhang, "Automatic waveform classification and arrival picking based on convolutional neural network," *Earth Space Sci.*, vol. 6, no. 7, pp. 1244–1261, 2019.
[183] Z. E. Ross, M.-A. Meier, and E. Hauksson, "P wave arrival picking and first-motion polarity determination with deep learning," *J. Geophysical Res.: Solid Earth*, vol. 123, no. 6, pp. 5120–5129, 2018.
[184] Z. He, P. Peng, L. Wang, and Y. Jiang, "Pickcapsnet: Capsule network for automatic p-wave arrival picking," *IEEE Geosci. Remote Sens. Lett.*, vol. 18, no. 4, pp. 617–621, Apr. 2021.
[185] I. Khan and Y.-W. Kwon, "P-detector: Real-time p-wave detection in a seismic waveform recorded on a low-cost MEMS accelerometer using deep learning," *IEEE Geosci. Remote Sens. Lett.*, vol. 19, pp. 1–5, Mar. 2022, Art. no. 3006305.
[186] M. Khandelwal and T. Singh, "Prediction of blast-induced ground vibration using artificial neural network," *Int. J. Rock Mechanics Mining Sci.*, vol. 46, no. 7, pp. 1214–1222, 2009.
[187] M. Monjezi, M. Ahmadi, M. Sheikhan, A. Bahrami, and A. Salimi, "Predicting blast-induced ground vibration using various types of neural networks," *Soil Dyn. Earthq. Eng.*, vol. 30, no. 11, pp. 1233–1236, 2010.
[188] M. Hasanipanah, M. Monjezi, A. Shahnazar, D. J. Armaghani, and A. Farazmand, "Feasibility of indirect determination of blast induced ground vibration based on support vector machine," *Measurement*, vol. 75, pp. 289–297, 2015.
[189] S. Dindarloo, "Peak particle velocity prediction using support vector machines: A surface blasting case study," *J. Southern Afr. Inst. Mining Metall.*, vol. 115, no. 7, pp. 637–643, 2015.
[190] E. Ghasemi, M. Ataei, and H. Hashemolhosseini, "Development of a fuzzy model for predicting ground vibration caused by rock blasting in surface mining," *J. Vib. Control*, vol. 19, no. 5, pp. 755–770, 2013.
[191] M. Iphar, M. Yavuz, and H. Ak, "Prediction of ground vibrations resulting from the blasting operations in an open-pit mine by adaptive neuro-fuzzy inference system," *Environ. Geol.*, vol. 56, no. 1, pp. 97–107, 2008.
[192] S. S. Moustafa, M. S. Abdalzaher, M. H. Yassien, T. Wang, M. Elwekeil, and H. E. A. Hafiez, "Development of an optimized regression model to predict blast-driven ground vibrations," *IEEE Access*, vol. 9, pp. 31826–31841, 2021.
[193] A. Chakravarty and S. Misra, "Unsupervised learning from three-component accelerometer data to monitor the spatiotemporal evolution of meso-scale hydraulic fractures," *Int. J. Rock Mechan. Mining Sci.*, vol. 151, 2022, Art. no. 105046.
[194] M. Bordbar, H. Aghamohammadi, H. R. Pourghasemi, and Z. Azizi, "Multi-hazard spatial modeling via ensembles of machine learning and meta-heuristic techniques," *Sci. Rep.*, vol. 12, no. 1, pp. 1–17, 2022.
[195] H. Seo, J. Kim, and B. Kim, "Machine-learning-based surface ground-motion prediction models for South Korea with low-to-moderate seismicity," *Bull. Seismological Soc. Amer.*, vol. 112, no. 3, pp. 1549–1564, 2022.
[196] M. S. Abdalzaher, S. S. Moustafa, M. Abd-Elnaby, and M. Elwekeil, "Comparative performance assessments of machine-learning methods for artificial seismic sources discrimination," *IEEE Access*, vol. 9, pp. 65524–65535, 2021.

[197] L. Linville, K. Pankow, and T. Draelos, "Deep learning models augment analyst decisions for event discrimination," *Geophysical Res. Lett.*, vol. 46, no. 7, pp. 3643–3651, 2019.
[198] X. Shang, X. Li, A. Morales-Esteban, and G. Chen, "Improving microseismic event and quarry blast classification using artificial neural networks based on principal component analysis," *Soil Dyn. Earthq. Eng.*, vol. 99, pp. 142–149, 2017.
[199] I. Niv, Y. Bregman, and N. Rabin, "Identification of mine explosions using manifold learning techniques," *IEEE Trans. Geosci. Remote Sens.*, vol. 60, pp. 1–13, Feb. 2022, Art. no. 5912313.
[200] X. Chai, G. Tang, S. Wang, R. Peng, W. Chen, and J. Li, "Deep learning for regularly missing data reconstruction," *IEEE Trans. Geosci. Remote Sens.*, vol. 58, no. 6, pp. 4406–4423, Jun. 2020.
[201] X. Chai, H. Gu, F. Li, H. Duan, X. Hu, and K. Lin, "Deep learning for irregularly and regularly missing data reconstruction," *Sci. Rep.*, vol. 10, no. 1, pp. 1–18, 2020.
[202] C.-Y. Wang, T.-C. Huang, and Y.-M. Wu, "Using LSTM neural networks for onsite earthquake early warning," *Seismological Res. Lett.*, vol. 93, no. 2A, pp. 814–826, 2022.
[203] X. Zhang, M. Zhang, and X. Tian, "Real-time earthquake early warning with deep learning: Application to the 2016 m 6.0 central Apennines, Italy earthquake," *Geophysical Res. Lett.*, vol. 48, no. 5, 2021, Art. no. 2020GL089394.
[204] A. Wibowo et al., "Earthquake early warning system using ncheck and hard-shared orthogonal multitarget regression on deep learning," *IEEE Geosci. Remote Sens. Lett.*, vol. 19, pp. 1–5, Mar. 2022, Art. no. 7502605.
[205] S. Nagendra et al., "Constructing a large-scale landslide database across heterogeneous environments using task-specific model updates," *IEEE J. Sel. Topics Appl. Earth Observ. Remote Sens.*, vol. 15, pp. 4349–4370, May 2022.
[206] Z. Fang, Y. Wang, R. Niu, and L. Peng, "Landslide susceptibility prediction based on positive unlabeled learning coupled with adaptive sampling," *IEEE J. Sel. Topics Appl. Earth Observ. Remote Sens.*, vol. 14, pp. 11581–11592, Nov. 2021.
[207] Y. Chen, D. Ming, X. Ling, X. Lv, and C. Zhou, "Landslide susceptibility mapping using feature fusion-based cpcnn-ml in lantau island, Hong Kong," *IEEE J. Sel. Topics Appl. Earth Observ. Remote Sens.*, vol. 14, pp. 3625–3639, Mar. 2021.
[208] H. Cai, T. Chen, R. Niu, and A. Plaza, "Landslide detection using densely connected convolutional networks and environmental conditions," *IEEE J. Sel. Topics Appl. Earth Observ. Remote Sens.*, vol. 14, pp. 5235–5247, May 2021.
[209] X. Gao, T. Chen, R. Niu, and A. Plaza, "Recognition and mapping of landslide using a fully convolutional densenet and influencing factors," *IEEE J. Sel. Topics Appl. Earth Observ. Remote Sens.*, vol. 14, pp. 7881–7894, Aug. 2021.
[210] G. Xu, Y. Wang, L. Wang, L. P. Soares, and C. H. Grohmann, "Feature-based constraint deep CNN method for mapping rainfall-induced landslides in remote regions with mountainous terrain: An application to Brazil," *IEEE J. Sel. Topics Appl. Earth Observ. Remote Sens.*, vol. 15, pp. 2644–2659, Mar. 2022.
[211] O. Ghorbanzadeh, S. R. Meena, H. S. S. Abadi, S. Tavakkoli Piralilou, L. Zhiyong, and T. Blaschke, "Landslide mapping using two main deep-learning convolution neural network streams combined by the Dempster–Shafer model," *IEEE J. Sel. Topics Appl. Earth Observ. Remote Sens.*, vol. 14, pp. 452–463, Dec. 2021.
[212] Q. Zhu, L. Chen, H. Hu, S. Pirasteh, H. Li, and X. Xie, "Unsupervised feature learning to improve transferability of landslide susceptibility representations," *IEEE J. Sel. Topics Appl. Earth Observ. Remote Sens.*, vol. 13, pp. 3917–3930, Jul. 2020.
[213] Y. Yi and W. Zhang, "A new deep-learning-based approach for earthquake-triggered landslide detection from single-temporal rapideye satellite imagery," *IEEE J. Sel. Topics Appl. Earth Observ. Remote Sens.*, vol. 13, pp. 6166–6176, Oct. 2020.
[214] J. Song, Y. Wang, Z. Fang, L. Peng, and H. Hong, "Potential of ensemble learning to improve tree-based classifiers for landslide susceptibility mapping," *IEEE J. Sel. Topics Appl. Earth Observ. Remote Sens.*, vol. 13, pp. 4642–4662, Aug. 2020.
[215] S. Chen, Z. Miao, L. Wu, and Y. He, "Application of an incomplete landslide inventory and one class classifier to earthquake-induced landslide susceptibility mapping," *IEEE J. Sel. Topics Appl. Earth Observ. Remote Sens.*, vol. 13, pp. 1649–1660, Apr. 2020.
[216] J. Schmidhuber, "Deep learning in neural networks: An overview," *Neural Netw.*, vol. 61, pp. 85–117, 2015.
[217] Y. LeCun, Y. Bengio, and G. Hinton, "Deep learning," *Nature*, vol. 521, no. 7553, pp. 436–444, 2015.
[218] M. S. Abdalzaher, M. Elwekeil, T. Wang, and S. Zhang, "A deep autoencoder trust model for mitigating jamming attack in IoT assisted by cognitive radio," *IEEE Syst. J.*, vol. 16, no. 3, pp. 3635–3645, Sep. 2022.
[219] X. Chai, G. Tang, S. Wang, K. Lin, and R. Peng, "Deep learning for irregularly and regularly missing 3-D data reconstruction," *IEEE Trans. Geosci. Remote Sens.*, vol. 59, no. 7, pp. 6244–6265, Jul. 2021.
[220] D. P. Kingma and J. Ba, "Adam: A method for stochastic optimization," 2015, *arXiv:1412.6980*.

Mohamed S. Abdalzaher (Senior Member, IEEE) received the B.Sc. (Hons.) and M.Sc. degrees from Ain Shams University, Cairo, Egypt, in 2008 and 2012, respectively, and the Ph.D. degree from the Electronics and Communications Engineering Department, Egypt-Japan University of Science and Technology, Madinet Borg Al Arab, Egypt, in 2016, all in electronics and communications engineering.

He is currently an Associate Professor with the Seismology Department, National Research Institute of Astronomy and Geophysics, Cairo, Egypt. He was a special Research Student with Kyushu University, Fukuoka, Japan, from 2015 to 2016. From April 2019 to October 2019, he joined the Center for Japan-Egypt Cooperation in Science and Technology, Kyushu University, where he was a Postdoctoral Researcher. His research interests include earthquake engineering, data communication networks, wireless communications, WSNs security, IoT, and deep learning.

Dr. Abdalzaher is a Guest Editor with *Energies Journal* and *Frontiers in Communications and Networks Journal*. He is also a TPC Member with Vehicular Technology Conference and International Japan-Africa Conference on Electronics, Communications and Computers and a reviewer of the *IEEE Internet of Things Journal*, *IEEE Systems Journal*, *IEEE Access*, *Transactions on Emerging Telecommunications Technologies*, *Applied Soft Computing*, *Journal of Ambient Intelligence and Humanized Computing*, and *IET Journals*.

Hussein A. Elsayed (Member, IEEE) (Member, IEEE) received the B.Sc. and M.Sc. degrees from the Electronics and Communications Engineering Department, Faculty of Engineering, Ain Shams University, Cairo, Egypt, in 1991 and 1995, respectively, and the Ph.D. degree from the Electrical Engineering Department, City University of New York, New York, NY, USA, in 2003, all in telecommunication networks.

Since graduated, he served in different positions and built both practical and theoretical skills in the area of telecommunication networks. He supervised and joined several telecommunication graduation, research, and lab/operational projects including service provider Network Operation Center (NOC). He is currently a Professor with the Electronics and Communications Engineering Department, Faculty of Engineering, Ain Shams University. His research interests include ad hoc networks, cognitive radio network (CRN), wireless sensor networks (WSN), medium access control (MAC), routing protocols, software-defined networks (SDN), device-to-device communication (D2D), and mobile systems, where he has a long list of publications.

Mostafa M. Fouda (Senior Member, IEEE) received the B.S. (as the valedictorian) and M.S. degrees in electrical engineering from Benha University, Egypt, in 2002 and 2007, respectively, and the Ph.D. degree in information sciences from Tohoku University, Japan, in 2011.

He is currently an Assistant Professor with the Department of Electrical and Computer Engineering, Idaho State University, Pocatello, ID, USA. He also holds the position of a Full Professor with Benha University. He was an Assistant Professor with Tohoku University and a Postdoctoral Research Associate with Tennessee Technological University, Cookeville, TN, USA. He has (co)authored more than 120 technical publications. His current research interests include cybersecurity, communication networks, signal processing, wireless mobile communications, smart health care, smart grids, AI, and IoT.

Dr. Fouda has guest-edited a number of special issues covering various emerging topics in communications, networking, and health analytics. He is currently serving on the editorial board of IEEE TRANSACTIONS ON VEHICULAR TECHNOLOGY (TVT) and *IEEE Access*. He has received several research grants including NSF-JUNO3.